Hydrol. Earth Syst. Sci. Discuss., https://doi.org/10.5194/hess-2018-26
Manuscript under review for journal Hydrol. Earth Syst. Sci.
Discussion started: 12 February 2018

Hydrology and Earth System Sciences
Discussions

Evaluation of Lacustrine Groundwater Discharge, Hydrologic Partitioning, and Nutrient Budgets in a Proglacial Lake in Qinghai-Tibet Plateau: Using ^{222}Rn and Stable Isotopes

Xin LUO[1, 2], Xing Xing Kuang[3], Jiu Jimmy Jiao[1, 2*], Sihai Liang[4], Rong Mao[1, 3], Xiaolang Zhang[1, 3], and Hailong Li[3]

[1]Department of Earth Sciences, The University of Hong Kong, P. R. China

[2]The University of Hong Kong, Shenzhen Research Institute (SRI), Shenzhen, P. R. China

[3]School of Environmental Science and Engineering, South University of Science and Technology of China (SUSTC), Shenzhen, China.

[4]School of Water Resources & Environment, China University of Geosciences, 29 Xueyuan Road, Beijing, China

Corresponding author: Jiu Jimmy Jiao (jjiao@hku.hk)

Department of Earth Sciences, The University of Hong Kong

Room 302, James Lee Science Building, Pokfulam Road, Hong Kong

Tel (852) 2857 8246; Fax (852) 2517 6912

Hydrol. Earth Syst. Sci. Discuss., https://doi.org/10.5194/hess-2018-26
Manuscript under review for journal Hydrol. Earth Syst. Sci.
Discussion started: 12 February 2018

Hydrology and Earth System Sciences
Discussions

Abstract

Proglacial lakes are good natural laboratories to investigate groundwater and glacier dynamics under current climate condition and to explore primary productivity under pristine lake status. This study conducted a series of investigations of ^{222}Rn, stable isotopes, nutrients and other hydrogeochemical parameters in Ximen Co Lake, a remote proglacial lake in the east of Qinghai-Tibet Plateau (QTP). A radon mass balance model was used to quantify the lacustrine groundwater discharge (LGD) of the lake, leading to an LGD estimate of 10.3 ± 8.2 mm d^{-1}. Based on the three end member models of stable ^{18}O and Cl^-, the hydrologic partitioning of the lake is obtained, which shows that groundwater discharge only accounts for 7.0 % of the total water input. The groundwater derived DIN and DIP loadings constitute 42.9 % and 5.5 % of the total nutrient loading to the lakes, indicating the significance of LGD in delivering disproportionate DIN into the lake. The primary productivity of the lake water is calculated to be 0.41 mmol C m^{-2} d^{-1}. This study presents the first attempts to evaluate the LGD and hydrologic partitioning in the glacial lake by coupling radioactive and stable isotopic approaches and the findings advance the understanding of nutrient budgets and primary productivity in the proglacial lakes of QTP. The study is also instructional in revealing the hydrogeochemical processes in proglacial lakes elsewhere.

Keywords: Proglacial lake; ^{222}Rn; lacustrine groundwater discharge; hydrologic partitioning; nutrient budgets; primary productivity

1. Introduction

High altitude and latitude areas are intensively influenced by the melting of glaciers due to climatic warming. Of particular importance are the proglacial areas, such as proglacial lakes and moraines, because they are particularly affected by climatic change induced glacier retreating and thawing of permafrost (Barry 2006, Heckmann et al. 2015, Slaymaker 2011). The proglacial lakes are usually located close to ice front of a glacier, ice cap or ice sheet, with the vicinity to the ice front sometimes defined as the areas with subrecent moraines and formed by the last significant glacier advances at the end of the Little Ice Age (Barry 2006, Harris et al. 2009, Heckmann et al. 2015, Slaymaker 2011). Proglacial lakes are located in the transition zones from glacial to non-glacial conditions, providing natural laboratories to explore hydrological processes, biogeochemical cycles and geomorphic dynamics under current climatic conditions (Dimova et al. 2015, Heckmann et al. 2015). Mountainous proglacial lakes, formed by glacial erosion and filled by melting glaciers, are widely distributed in the Qinghai-Tibet Plateau (QTP), especially along the substantial glacier retreating areas of Himalaya Mountains (MT.), Qilian MT.,

Hydrol. Earth Syst. Sci. Discuss., https://doi.org/10.5194/hess-2018-26
Manuscript under review for journal Hydrol. Earth Syst. Sci.
Discussion started: 12 February 2018

64 Tienshan MT., etc. Characterized by higher elevations, small surface areas but
65 relatively large depths, mountainous proglacial lakes in QTP lack systematic
66 field-based hydrological studies due to their remote locations and difficulty in
67 conducting field work (Bolch et al. 2012, Farinotti et al. 2015, Yao et al. 2012).

68 There has been extensive recognition of the importance of groundwater discharge
69 to various aquatic systems for decades (Dimova and Burnett 2011, Johannes 1980,
70 Valiela et al. 1978). Very recently, the topic of 'lacustrine groundwater discharge
71 (LGD)', which is comprehensively defined as groundwater exfiltration from lake
72 shore aquifers to lakes (Blume et al. 2013, Lewandowski et al. 2015, Lewandowski et
73 al. 2013, Rosenberry et al. 2015), has been introduced. LGD is analogous of in
74 submarine groundwater discharge (SGD) in coastal environments. LGD plays a vital
75 role in lake hydrologic partitioning, which is defined as the separation of groundwater
76 discharge/exfiltration, riverine inflow, riverine outflow infiltration, surface
77 evaporation and precipitation for the hydrological cycle of the lake (Good et al., 2015).
78 LGD also serves as an importance component in delivering solutes to lakes since
79 groundwater is usually concentrated in nutrients, CH_4, dissolved inorganic/organic
80 carbon (DIC/DOC) and other geochemical components (Belanger et al. 1985, Dimova
81 et al. 2015, Lecher et al. 2015, Paytan et al. 2015). Nutrients and carbon loading from
82 groundwater greatly influences ratios of dissolved inorganic nitrogen (DIN) to

dissolved inorganic phosphate (DIP) (referred as N: P ratios thereafter), ecosystem structure and the primary productivity of the lake aquatic system (Belanger et al. 1985, Hagerthey and Kerfoot 1998, Nakayama and Watanabe 2008).

LGD studies utilize various methods including direct seepage meters (Lee 1977, Shaw and Prepas 1990), geo-tracers such as radionuclides, stable ^{2}H and ^{18}O isotopes (Gat 1995, Kluge et al. 2007, Kraemer 2005, Lazar et al. 2008), heat and temperature (Liu et al. 2015, Sebok et al. 2013), numerical modeling (Smerdon et al. 2007, Winter 1999, Zlotnik et al. 2009, Zlotnik et al. 2010) and remote sensing (Anderson et al. 2013, Lewandowski et al. 2013, Wilson and Rocha 2016). Recently, some researchers started to investigate groundwater dynamics in peri- and proglacial areas, mostly based on the approaches of numerical modeling (Andermann et al. 2012, Lemieux et al. 2008a, Lemieux et al. 2008b, Lemieux et al. 2008c, Scheidegger and Bense 2014). However, the quantification of groundwater and surface water exchange in proglacial lakes is still challenging due to limited hydrogeological data and extremely seasonal variability of aquifer permeability (Callegary et al. 2013, Dimova et al. 2015, Xin et al. 2013).

^{222}Rn, a naturally occurring inert gas nuclide highly concentrated in groundwater, can be more applicable in fresh aquatic systems and has been widely used as a tracer to quantify groundwater discharge in fresh water lakes (Corbett et al. 1997, Dimova et

al. 2015, Dimova and Burnett 2011, Dimova et al. 2013, Kluge et al. 2007, Kluge et al. 2012, Luo et al. 2016, Schmidt et al. 2010) and terrestrial rivers and streams (Batlle-Aguilar et al. 2014, Burnett et al. 2010, Cook et al. 2006, Cook et al. 2003). Of particular interest are investigations of temporal ^{222}Rn distribution in lakes, since it can be used to quantify groundwater discharge and reflect the locally climatological dynamics (Dimova and Burnett 2011, Luo et al. 2016). Temporal radon variations give high resolution estimates of groundwater discharge to lakes over diel cycles, allowing evaluation of LGD and the associated chemical loadings. However, there has been no study of radon-based groundwater discharge in mountainous proglacial lakes, especially for those lakes in the QTP.

This study aims to investigate the groundwater surface water interactions for the proglacial lake of Ximen Co, by estimating the LGD and evaluating the hydrologic partitioning of the lake. LGD is estimated with ^{222}Rn mass balance model, and the hydrologic partitioning of the lake is obtained with the three endmember model coupling the mass balance of water, stable isotopes and Cl^-. Then, LGD derived nutrients are estimated and the nutrient budgets of the lake are depicted. Finally, primary productivity of the lake water is calculated based on the nutrient budgets. This study, to our knowledge, makes the first attempt to quantify the LGD, hydrologic partition, and groundwater borne nutrients of the proglacial lake in QTP

and elsewhere via the approach integrating multiple tracers. This study provides insights of hydrologic partitioning in a typical mountainous proglacial lake under current climate condition and reveals groundwater borne chemical loadings in this proglacial lake in QTP and elsewhere.

2. Methodology

2.1 Site descriptions

The Nianbaoyeze MT., located at the eastern margin of the QTP and being the easternmost part of NW-SW trending Bayan Har Shan, is situated at the main water divide of the upper reaches of Yellow River and Yangtze River (Figure 1). With a peak elevation of 5369 m, the mountain rises about 500-800 m above the surrounding peneplain and displays typical Pleistocene glacial landscapes such as moraines, U-shaped valleys and cirques (Lehmkuhl 1998, Schlutz and Lehmkuhl 2009, Wischnewski et al. 2014). The present snow line is estimated to be at an elevation of 5100 m (some updated references) (Schlutz and Lehmkuhl 2009). Controlled by the South Asia and East Asia monsoons, the mountain has an annual precipitation of 975 mm in the southern part and 582 mm in the northwestern part, with 80 % occurring during May and October (Yuan et al. 2014, Zhang and Mischke 2009). The average temperature gradient is about 0.55 ^{o}C per 100 m, and the closest weather station,

Hydrol. Earth Syst. Sci. Discuss., https://doi.org/10.5194/hess-2018-26
Manuscript under review for journal Hydrol. Earth Syst. Sci.
Discussion started: 12 February 2018

140 locating in Jiuzhi town (N: 33.424614°, E: 101.485998) at the lower plains of the
141 mountain, recorded a mean annual temperature of 0.1 ^{o}C. Snowfalls occur in nearly
142 10 months of the entire year and there is no free-frost all year around (Böhner 1996,
143 2006, Schlutz and Lehmkuhl 2009). The precipitation, daily bin-averaged wind speed
144 and temperature in Aug, 2015 were recorded to be 90 mm, .7 m s^{-1} and 9.5 ^{o}C from
145 Jiuzhi weather station (Figure 2). The water surface evaporation was recorded to be
146 1429.8 mm in 2015 from Jiuzhi weather station.

147 Among the numerous proglacial lakes developed in the U-shaped valleys of the
148 Nianbaoyeze MT., Ximen Co lake is located at the northern margin of the mountain
149 with an elevation of 4030 m asl, and is well studied and easily accessible (Lehmkuhl
150 1998, Schlutz and Lehmkuhl 2009, Yuan et al. 2014, Zhang and Mischke 2009). The
151 lake was formed in a deep, glacially eroded basin with a catchment area of 50 km^2,
152 and has a mean and a maximum depth of 40 m and 63.2 m, and a surface area of 3.6
153 km^2. The vegetation around the lake is dominated by pine meadows with dwarf shrubs,
154 rosette plants and alpine cushion (Schlutz and Lehmkuhl 2009, Yuan et al. 2014,
155 Zhang and Mischke 2009). Mostly recharged by the glacial and snowpack melting
156 water and regional precipitation, the lake is stratified with an epilimnion depth about
157 4.4 m in the summer time. The lake is usually covered by ice in the winter time
158 (Zhang and Mischke 2009). The superficial layer within the U-shaped valley is

159 characterized by peat, clay and fluvial gravels with a depth about 1-3.5 m.
160 Discontinuous and isolated permafrost is present at the slope of the valley above the
161 elevation of about 4150 m. The maximum frozen depth is about 1.5 m for the seasonal
162 frozen ground around the lake. The seasonal frozen ground serves as an unconfined
163 aquifer during the unfrozen months from July to October, and groundwater discharges
164 into the epilimnion of the lake (Schlutz and Lehmkuhl 2009, Wang 1997, Zhang and
165 Mischke 2009).
166
167 2.2 Sampling and field analysis
168 The field campaign to Ximen Co Lake was conducted from August, 2015, when it is
169 warm enough to take the water samples of different origins as the studied site is
170 seasonally frozen. A ^{222}Rn continuous monitoring station was setup at the southeast
171 part of the lake, which is fairly flat for setting up our tent and monitoring system.
172 Surface water samples were collected around the lake, rivers at the upstream and
173 downstream. Porewater samples were collected at one side of the lake as the other
174 side is steep and rocky. The basic water quality parameters of conductivity (EC),
175 dissolved oxygen (DO), TDS, ORP, pH in the water were recorded with the
176 multi-parameter meter (HANNA, Co.). Relative humidity was recorded with a
177 portable thermo-hydrometer (KTH-2, Co.). Lake water samples were taken with a

178 peristaltic pump into 2.5 L glass bottles for ^{222}Rn measurement with the Big Bottle
179 system (Durridge, Co.). Surface water samples were filtered with 0.45 μm filters
180 (Advantec, Co.) in situ and taken into 5 ml, 15 ml, 15 ml and 50 ml Nalgene
181 centrifugation tubes for stable isotope, major anion, cation and nutrient analysis.
182 Porewater samples were taken from the lakes shore aquifers with a push point sampler
183 (M.H.E, Co.) connected to peristaltic pump (Solinst, Co.) (Luo et al. 2014, Luo et al.
184 2016). 100 ml raw surface water or porewater was titrated with 0.1 μM H_2SO_4
185 cartridge (Hach, Co.) in situ to measure total alkalinity (Hasler et al. 2016, Warner et
186 al. 2013, White et al. 2016). Porewater was filtered with 0.45 μm syringe filters
187 (Advantec, Co.) in situ and taken into 5 ml, 15 ml, 15 ml and 50 ml Nalgene
188 centrifugation tubes for stable isotope, major anion, cation and nutrient analysis. 250
189 ml porewater was taken for ^{222}Rn measurement with RAD7 H_2O (Durridge, Co.)
190 Samples for major cation analysis were acidified with distilled HNO_3 immediately
191 after the sampling.

192 ^{222}Rn continuous monitoring station was set up at the northwest of the lake, close
193 to the downstream of the lake (Figure 1b). Lake water (about 0.5 m) was pumped with
194 a DC pump (12 V) driven by lithium batteries (100 Ah) and sprinkled into the
195 chamber of RAD7 AQUA with a flow rate > 2 min L^{-1}, where ^{222}Rn in water vapor
196 was equilibrated with the air ^{222}Rn. The vapor in the chamber was delivered into two

large dry units (Drierite, Co) to remove the moisture and circulated into RAD7 monitor, where ^{222}Rn activities were recorded every 5 mins. A temperature probe (HOBO$^{@}$) was insert into the chamber to record the temperature of the water vapor. The monitoring was performed from 11: 31 am, Aug 22nd to 6: 30 am, Aug 24th, 2015. During the period of 1:50-4:30 pm on Aug 22nd, a sudden blizzard occurred, leading to an hourly precipitation about 0.6 mm to the lake area. Daily and hourly climatological data such as wind speed, air temperature and precipitation were retrieved from the nearest weather station in Jiuzhi town (N: 33.424614°, E: 101.485998). Water level and temperature fluctuations were recorded with a conductivity-temperature-depth diver (Schlumberger, Co.) fixed at about 20 cm below the lake surface and calibrated with local atmospheric pressure recorded by a baro-diver (Schlumberger, Co.) above the lake. To correct for dissolved ^{226}Ra supported ^{222}Rn, one radium sample was extracted from 100 L lake water with MnO_2 fiber as described elsewhere (Luo et al. 2014, Moore 1976).

2.3 Chemical analysis

Major ions were measured with ICS-1100 (Dionex. Co.) in the Department of Earth Sciences, the University of Hong Kong. The uncertainties of the measurements are less than 5 %. Nutrients, DIN and DIP were analyzed with flow injection analysis

equipped with auto-sampler (Lachat. Co.) in the School of Biological Sciences, the University of Hong Kong. Stable ^{18}O and ^{2}H isotopes were measured with MOA-ICOS laser absorption spectrometer (Los Gatos Research (LGR) Triple Isotope Water Analyzer (TIWA-45EP)) at State Key Laboratory of Marine Geology, Tongji University, Shanghai. The stable isotopic standards and the recovery test has been fully described elsewhere (Luo et al., 2017). The measurement uncertainty is better than 0.1 % for ^{18}O and 0.5 % for ^{2}H. ^{226}Ra was detected with RAD7 with the method described elsewhere (Kim et al. 2001, Lee et al. 2012)

2.4 Radon transient model

Previous studies employed a steady state radon-222 mass balance model to quantify LGD to lentic system such as lakes and wetlands (Dimova and Burnett 2011, Luo et al. 2016). This model assumes that radon input derived from groundwater inflow, diffusion and river inflow are balanced by the radon losses of atmospheric evasion, decay and river outflow. However, recently studies revealed that the steady state is mainly reached after 2-15 days of constant metrological conditions, and mostly lentic system can be not be treated as steady state due to rapid radon-222 degassing to the atmosphere driven by wind-induced turbulence (Gilfedder et al., 2015; Dimova and Burnett, 2011).

Hydrol. Earth Syst. Sci. Discuss., https://doi.org/10.5194/hess-2018-26
Manuscript under review for journal Hydrol. Earth Syst. Sci.
Discussion started: 12 February 2018

235 Ximen Co lake is demonstrated to be highly stratified with an epilimnion of 4.4
236 m (Zhang and Mischke 2009). The lake was formed by glacier erosion and the
237 lakebed is characterized by granite bedrock with a thin sedimentary clay layer.
238 Previous studies have indicated that sediment with a thickness of 0.7-3.3 m has been
239 developed on the bedrock and forms the lake shore aquifer, which consists of clay,
240 soils and gravels (Schlutz and Lehmkuhl 2009). Porewater sampled in the aquifer
241 immediately behind the lake shore can well represent groundwater discharging into
242 the lake, as suggested previously (Lewandowski et al. 2015, Rosenberry et al. 2015,
243 Schafran and Driscoll 1993). LGD has been widely considered to occur within the
244 first few meters of the lake shore (Lee et al. 1980, Rosenberry et al. 2015, Schafran
245 and Driscoll 1993) and groundwater is considered to predominately discharge into the
246 epilimnion since deep groundwater flow is highly limited by the Precambrian bedrock
247 (Einarsdottir et al., 2016). Therefore, ^{222}Rn mass balance model is established to
248 quantify LGD to the epilimnion from the lake shore. Due to negligible hydrological
249 connection between the epilimnion and hypolimnion, LGD for the lake can be
250 quantified with ^{222}Rn mass balance model for the epilimnion.

251 The governing equation of radon-222 transient mass balance model within a 1 x
252 1 x z cm (where z is the depth in cm) can be expressed as (Gilfedder et al. 2015):

253 $$z\frac{\partial I_{\mathrm{w}}}{\partial \mathrm{t}} = F_{gw} + (I_{^{226}Ra} - I_{\mathrm{w}}) \times z \times \lambda_{222} + F_{diff} - F_{atm} \qquad (1)$$

Hydrol. Earth Syst. Sci. Discuss., https://doi.org/10.5194/hess-2018-26
Manuscript under review for journal Hydrol. Earth Syst. Sci.
Discussion started: 12 February 2018

where F_{gw}, F_{diff}, F_{atm} [Bq m^{-2} d^{-1}] are ^{222}Rn loadings from LGD, water-sediment diffusion and water-air evasion, respectively; z [m] is the lake water level depth recorded by the diver. λ_{222} is the decay constant of ^{222}Rn with a value of 0.186 d^{-1}. $\lambda_{222} \times I_{^{226}Ra}$ and $\lambda_{222} \times I_w$ account for the production and decay of ^{222}Rn [Bq m^{-2} d^{-1}] in the water column, respectively. I_w and $I_{^{226}Ra}$ [Bq m^{-2}] represent ^{222}Rn and ^{226}Ra inventories in the epilimnion, and are expressed as: $I_w = H \times C_w$ and $I_{^{226}Ra} = H \times C_{^{226}Ra}$, respectively; where H [m] is the depth of the epilimnion; C_w and $C_{^{226}Ra}$ is the ^{222}Rn and ^{226}Ra activity [Bq m^{-3}], respectively.

The model is valid under the following assumptions: 1) The epilimnion is well mixed which is the actual condition for most natural boreal and high altitude glacial lakes (Åberg et al. 2010, Zhang and Mischke 2009). 2) ^{222}Rn input from riverine water inflow, and loss from the lake water outflow and infiltration into the lake shore aquifer is negligible compared to the groundwater borne ^{222}Rn, because ^{222}Rn concentration of groundwater is 2-3 orders of magnitude larger than that lake water (Dimova and Burnett 2011, Dimova et al. 2013). Generally, ^{222}Rn in the epilimnion is sourced from LGD and decay input from parent isotope of ^{226}Ra under secular equilibrium, and is mainly lost via atmospheric evasion and radioactive decay.

F_{atm} is the key sinking component of the transient model and is finally a function of wind speed and water temperature, both of which are temporal variant variables

Hydrol. Earth Syst. Sci. Discuss., https://doi.org/10.5194/hess-2018-26
Manuscript under review for journal Hydrol. Earth Syst. Sci.
Discussion started: 12 February 2018

(Supplementary information). Lake water level z is also a temporal variant variable which represents the fluctuations of water volume of the epilimnion. This equation is discretized by the forward finite difference method, and the groundwater flux at each time step can be solved as follow

$$[{}^{222}Rn_{t+\Delta t}] = \frac{[z \times {}^{222}Rn_t + [F_{diff} + F_{gw} - F_{atm} - {}^{222}Rn_t \times \lambda \times z] \times \Delta t}{z} \quad (2)$$

where ${}^{222}Rn_{t+\Delta t}$ and ${}^{222}Rn_{t+\Delta t}$ [Bq m^{-3}] is the ^{222}Rn activity at current time step and at the previous time steps, respectively, and Δt [min] is the time step. With the inverse calculation based on Equation (4), the groundwater inflow at each time step can be obtained. However, large errors of the final LGD calculation will be induced by even a small amount of noise in the measured ^{222}Rn data due to the ${}^{222}Rn_{t+\Delta t} - {}^{222}Rn_t$ term being with the measure uncertainty. To reduce the random errors of the measured ^{222}Rn concentrations, the time window with a width of 1 hour is proposed to smooth the curve (Supplementary information).

3. **Results**

3.1 Time series data

Figure 2 shows the basic climatological parameters of the lake catchment during the campaign month. There are discrete rainfall events occurring throughout the month with an average rainfall of 3.1 mm d^{-1}. The temperature throughout the month ranges from 5.0 – 12.5 ^{o}C within an average of 9.3 ^{o}C. The daily averaged wind speed

293 generally ranges from 0.7 – 2.5 m s^{-1}, with an average of 1.7 m s^{-1}. ^{222}Rn temporal
294 distribution and other time series data are shown in Figure 3a and listed in
295 Supplementary Table 1. Generally, ^{222}Rn concentration varies from 32.2 to 273 Bq m^{-3},
296 with an average of 144.2 ± 27.7 Bq m^{-3}. ^{222}Rn over the monitoring period shows
297 typical diel cycle, much higher at nighttime and lower in the day time. Figures 3b-3d
298 shows the time series data of temperature (5 mins interval), nearshore lake water level
299 (1 min interval), and wind speed (1 hour interval). Temperature and lake water level
300 also show typical diel cycles, but with antiphase fluctuations with each other.
301 Temperature is higher during the daytime and lower at nighttime. However a sudden
302 decrease of temperature was recorded due to the sudden blizzard (Figure 3b). Water
303 level is higher at nighttime and lower during the daytime, with a strong fluctuation
304 due to the turbulence caused by the blizzard (Figure 3c). The variability might reflect
305 the dynamics of groundwater input and surface water inflow. The air temperature of
306 the lake area is in phase with the water temperature. Wind speed is normally higher
307 during the daytime and lower at nighttime (Figure 3d).

308 The variation of ^{222}Rn is nearly in antiphase with the fluctuations of lake water
309 temperature and air temperature, indicating that the dominated controlling factors
310 of ^{222}Rn fluctuations are water temperature and wind speed (Figure 3a). This
311 phenomenon is reasonable as lake water ^{222}Rn is predominately lost via atmospheric

312 evasion, which is the function of wind speed and water temperature (Dimova et al.
313 2015, Dimova and Burnett 2011, Dimova et al. 2013). High water temperature and
314 wind speed leads to elevated atmospheric evasion and causes the decline of ^{222}Rn
315 concentration in the lake water. However, there is a sudden reduction of radon activity
316 from 2: 00 pm to 4: 00 pm on Jul 22nd, 2015, when the snow event led to a sudden
317 decrease of water temperature, increase of wind speed, and large surface water
318 turbulence as indicated by water level fluctuations (Figures 3a-3d). ^{222}Rn in the
319 porewater is 2-3 orders of magnitude larger than ^{222}Rn in the lake water, suggesting
320 that ^{222}Rn is an ideal tracer to estimate the LGD (Supplementary Table 1). ^{222}Rn
321 concentrations in surface water range from 22.2 to 209 Bq m^{-3}, with an average of
322 92.5 Bq m^{-3} (n = 12), which is in the range of ^{222}Rn continuous monitoring results,
323 suggesting reliable ^{222}Rn measurements (Supplementary Table 2).
324
325 3.2 Geochemical results
326 The results of major ions, nutrients and stable isotopes in different water end
327 members are shown in Figures 4 and 5. Cl^- ranges from 0.6 to 2.1 mg L^{-1} in the
328 surface water (including riverine inflow water, lake water and downstream water), 0.4
329 to 2.7 mg L^{-1} in porewater and has a much higher concentration of 5.9 mg L^{-1} in
330 rainfall water. Na^+ ranges from 1.6 to 3.4 mg L^{-1} in the surface water, 1.2 to 4.4 mg

331 L^{-1} in porewater and has a concentration of 4.4 mg L^{-1} in rainfall water. SO_4^{2-} ranges
332 from 1.2 to 2.3 mg L^{-1} in the surface water, 0.4 to 1.7 mg L^{-1} in porewater and has a
333 significant low concentration of 0.01 mg L^{-1} in rainfall water. Ca^{2+} ranges from 3.0 to
334 12.4 mg L^{-1} in lake water, 3.4 to 12.5 mg L^{-1} in porewater and has a significant high
335 concentration of 20.5 mg L^{-1} in rainfall water. Other concentrations of major ions are
336 listed in Supplementary Table 2. As shown in Figure 4d and Supplementary Table 2,
337 $\delta^{18}O$ in the lake water ranges from - 13.06 ‰ to - 12.11 ‰, with an average of -
338 12.41 ‰ (n = 7), and $\delta^{2}H$ ranges from - 91.83 ‰ to - 87.47 ‰, with an average of -
339 89.0 ‰ (n = 7). $\delta^{18}O$ in the riverine inflow water ranges from - 13.44 ‰ to - 13.29 ‰,
340 with an average of – 13.37 ‰ (n = 2), and $\delta^{2}H$ ranges from - 93.25 ‰ to – 91.92 ‰,
341 with an average of - 92.59 ‰ (n = 2). $\delta^{18}O$ in the downstream water ranges from -
342 12.51 ‰ to - 12.18 ‰, with an average of - 12.35 ‰ (n = 3), and $\delta^{2}H$ ranges from -
343 88.96 ‰ to - 87.1 ‰, with an average of - 87.98 ‰ (n = 3). $\delta^{18}O$ in the porewater
344 ranges from - 12.66 ‰ to - 11.52 ‰, with an average of - 11.97 ‰ (n = 8), and $\delta^{2}H$
345 ranges from – 91.3 ‰ to -82.87 ‰, with an average of - 85.5 ‰ (n = 8). DIN in the
346 surface water (including riverine inflow water, lake water and downstream water)
347 range from 6.6 to 16.9 μM, with an average of 10.3 μM, and DIP from 0.36 to 0.41
348 μM, with an average of 0.38 μM. The concentrations of DIN for the porewater range
349 from 0.7 to 358.8 μM, with an average of 92.8 μM, and DIP from 0.18 to 0.44 μM

350 with an average of 0.31 μM (Figure 5).

351

352 **4. Discussion**

353 4.1 Proglacial hydrologic processes and geochemical implications

354 Generally, major ion concentrations in the lake water and porewater of Ximen
355 Co lake are significantly lower than those in main rivers, streams and other tectonic
356 lakes in the QTP (Wang et al. 2010, Wang et al. 2016b, Yao et al. 2015), and are
357 similar to those of snow and glaciers (Liu et al. 2011), suggesting that the lake water
358 is mainly originated from glacier and snow melting. Ion concentrations in the lake and
359 porewater of Ximen Co lake are much lower than those of rainfall collected in Jiuzhi
360 town. This suggests that lake water is less influenced by precipitation (Figures 4a-4c).
361 The concentrations of major ions in the porewater are high compared to the lake water,
362 indicating weathering affects from the aquifer grains. The ratios of Ca^{2+}/Na^{+} in the
363 porewater and groundwater is >1, also suggesting influences of weathering digenesis
364 of major ions from the seasonal frozen ground at the lake shore aquifer (Wang et al.
365 2010, Weynell et al. 2016, Yao et al. 2015).

366 The isotopic compositions of the lake water and porewater are significantly
367 isotopic depleted, with values close to the compositions of glaciers and surface snow
368 in the QTP, suggesting the lake is dominantly recharged from snow and glacier

melting (Cui et al. 2014, Wang et al. 2016a, Zongxing et al. 2015). The relation of $\delta^{18}O$ versus $\delta^{2}H$ for the lake water is $\delta^{2}H = 4.25 \times \delta^{18}O - 35.99$, with a slope much lower than that of the global meteoric water line (GMWL) (Figure 4d), suggesting the effects of lake surface evaporation. The relation of $\delta^{18}O$ versus $\delta^{2}H$ for the porewater is $\delta^{2}H = 6.93 \times \delta^{18}O - 2.67$, overall on GWML (Figure 4d). Deuterium excesses is defined as $\Delta D = \delta D - 8 \times \delta^{18}O$ (Dansgaard 1964). The value of ΔD is dependent on airmass origins, altitude effect and the kinetic effects during evaporation (Hren et al. 2009). Global meteoric water has a ΔD of + 10 ‰. In QTP, glacier/snowpack melting water usually has large positive ΔD, while the precipitations derived from warm and humid summer monsoon has lower ΔD (Ren et al. 2017, Ren et al. 2013). In this study, ΔD of surface water, lake and porewater ranges from + 37.1 to + 41.2 ‰, closed to the glacier melting water but much larger than that of the local precipitation of + 29.72 ‰, This indicates the stream and lake water are mainly originated from glacial/snowpack melting rather than precipitation (Gat 1996, Lerman et al. 1995, Wang et al. 2016a). The slopes of $\delta^{18}O$ versus $\delta^{18}O$ in lake water and porewater are 4.25 and 6.93, both of which are lower than that of GMWL due to surface evaporation. Lake water is more intensively influenced by evaporation compared to porewater. The plots of $\delta^{18}O$ versus Cl^{-}, and $\delta^{2}H$ versus Cl^{-} are well clustered for porewater end member (orange area), lake water end member (blue area), riverine inflow water end

Hydrol. Earth Syst. Sci. Discuss., https://doi.org/10.5194/hess-2018-26
Manuscript under review for journal Hydrol. Earth Syst. Sci.
Discussion started: 12 February 2018

member (yellow area), and precipitation water (Figures 4e and 4f), suggesting stable $\delta^{18}O$ and $\delta^{2}H$ isotopes and Cl^- can serve as tracers to quantify the hydrologic partitioning of the lake by setting three endmember models.

The concentrations of DIN and DIP are all within the ranges of other glacial melting water and proglacial lake water (Hawkings et al. 2016, Hodson 2007, Hodson et al. 2005, Hudson et al. 2000, Tockner et al. 2002). Briefly, rainfall and upstream lake water such as YN-4 has the highest DIN concentration, indicating the glacier melting and precipitation could be important DIN sources in proglacial areas (Anderson et al. 2017, Dubnick et al. 2017). DIN in porewater is overall higher compared to the lake water, suggesting the porewater to be DIN effective source; and DIP concentrations is higher in the lake water compared to porewater, suggesting the porewater is a DIP sink (Figure 5). The N: P ratios in the lake water and porewater are averaged to be 27.1 and 320.5, respectively, both much larger than the Redfield Ratio (N: P = 16:1) in water and organism in most aquatic system and within the range of other proglacial lakes (Anderson et al. 2017). This also suggests that the lake water and porewater are under phosphate limited condition. N: P ratio in the rainfall water is 30.4, similar to the lake water. The average N: P ratio of porewater is much higher than that of lake water, indicting DIN enrichment in the lake shore aquifers (Figure 5). In pristine groundwater, NO_3^- is the predominated form of N and is highly mobile

407 within the oxic aquifers, leading to much higher DIN concentrations in the porewater;
408 DIP has high affinity to the aquifer grains, resulting in much lower DIP concentrations
409 in the porewater (Lewandowski et al. 2015, Rosenberry et al. 2015, Slomp and Van
410 Cappellen 2004). Thus, in analogous to surface runoff from glacier/snowpack melting,
411 LGD can be also regarded as an important source for the proglacial lakes. Because of
412 very high DIN and N: P ratios in the porewater, a relatively small portion of LGD
413 delivers considerable nutrients into the glacial lake, shifting the aquatic N: P ratios
414 and affecting the proglacial aquatic ecosystem (Anderson et al. 2017).
415
416 4.2 Estimation of LGD
417 Figure 6a shows all the sinks and sources of radon with the epilimnion of the lake.
418 Within ^{222}Rn transient mass balance model, the dominant ^{222}Rn loss is atmospheric
419 degassing/evasion. Generally, ^{222}Rn degassing rate is the function of the radon-222
420 concentration gradient at the water-air interface and the parameter of gas piston
421 velocity *k*, which is finally the function of wind speed and water temperature (Dimova
422 and Burnett 2011, Gilfedder et al. 2015). To evaluate ^{222}Rn evasion rate, this study
423 employs the widely used method proposed by MacIntyre et al. (1995) which is also
424 detailed described in Supplementary Information. Based on the field data of ^{222}Rn
425 concentration in the lake water, wind speed and temperature log, the radon degassing

426 rate is calculated in a range of 0.8 to 265.2 Bq m^2 d^{-1}, with an average 42.0 of Bq m^2
427 d^{-1}.

428 In addition to the atmospheric loss and sedimentary diffusion inputs, ^{222}Rn is also
429 sinked via radioactive decay, and sourced from decay of parent isotope of ^{226}Ra. The
430 decay loss of ^{222}Rn fluctuates in phase with the distribution of ^{222}Rn concentration
431 monitored by RAD 7 AQUA. The equations to estimate benthic fluxes are shown in
432 supplementary information. The decay loss is calculated to be 26.4 to 223.4 Bq m^{-2} d^{-1},
433 with an average of 118.0 ± 22.7 Bq m^{-2} d^{-1}. ^{226}Ra concentration is 0.01 Bq m^{-3} for the
434 lake water. Under secular equilibrium, the ^{226}Ra decay input can be calculated by
435 multiplying ^{226}Ra concentration in the lake water with λ_{222} (Corbett et al. 1997, Kluge
436 et al. 2007, Luo et al. 2016). ^{226}Ra decay input is calculated to be 0.83 Bq m^{-2} d^{-1},
437 which is significantly low compared to other ^{222}Rn sources to the epilimnion.

438 With the obtained sinks and sources of ^{222}Rn in the lake, and the constants given in
439 Table 1, LGD rate can be obtained by dividing the groundwater derived ^{222}Rn with its
440 concentration in groundwater endmember. The obtained LGD rate, ranges from -23. 7
441 mm d^{-1} to 90.0 mm d^{-1}, with an average of 10.3 ± 8.2 mm d^{-1} (Figure 7) The LGD rate
442 range is relatively less than the daily lake water level variations (≈ 50 mm), indicating
443 that the lake water level variation could be a combined effect of surface runoff and
444 LGD (Hood et al. 2006). The negative values of LGD rate reflect the return

Hydrol. Earth Syst. Sci. Discuss., https://doi.org/10.5194/hess-2018-26
Manuscript under review for journal Hydrol. Earth Syst. Sci.
Discussion started: 12 February 2018

groundwater flow due to infiltration into the porewater. Normally, the dominant values are positive, indicating LGD rate is significant compared to water infiltrations into lakeshore aquifer. The temporal variation of LGD rate could be attributed to the fluctuations of the hydraulic gradient in the proglacial areas (Hood et al. 2006, Levy et al. 2015). As indicated by ΔD (mostly > 10) of surface water, the lake and the upstream water is considered to be mainly recharged from glacial/snowpack melting rather other precipitations.

To assess the magnitude of uncertainty of ^{222}Rn transient model, the sensitivity of estimated LGD to changes in other variables is examined. A sensitivity coefficient *f* is proposed to evaluate this uncertainty according to Langston et al. (2013)

$$f = (\Delta F_{LGD} / F_{LGD}) / (\Delta y_i / y_i) \quad (3)$$

where ΔF_{LGD} is the amount of change in F_{LGD} from the original value. Δy_i is the amount of change in the other variable of y_i from the original value. Thus, higher *f* indicates a large uncertainty of final LGD estimate. The uncertainty mainly stems from ^{222}Rn measurements in different water endmembers, the atmospheric loss and water level record. The uncertainties of ^{222}Rn measurement are about 10 % and 15-20 % in groundwater and lake water endmember, respectively. The uncertainty of atmospheric loss is derived from uncertainty of ^{222}Rn in lake water (with an uncertainty of 15-20 %), temperature (with an uncertainty ≈ 5 %) and wind speed

464 (with an uncertainty ≈ 5 %). Thus, the final LGD estimate has an uncertainty of
465 35-40 %.
466
467 **4.3 Hydrologic partitioning**
468 Compared to the groundwater labeled radionuclide of ^{222}Rn, stable $^{18}O/^{2}H$
469 isotopes are advantageous in the investigation of evaporation processes due to their
470 fractionations from water to vapor and have been widely used to investigate the
471 hydrologic cycle of lakes in various environments (Gat 1995, Gibson et al. 1993,
472 Gonfiantini 1986, Stets et al. 2010). With the field data of stable isotopic composition
473 and Cl^- concentrations in different water end members, groundwater input, surface
474 water input, lake water outflow and infiltration, and evaporation can be partitioned by
475 coupling stable isotopic mass balance model with Cl^- mass balance model (Figure 6b).
476 The model, consisting of the budgets of stable isotopes and Cl^-, and water masses
477 for the epilimnion, is used to quantify riverine inflow, lake water outflow and
478 infiltration, and evaporation (Gibson et al. 2016, LaBaugh et al. 1995, LaBaugh et al.
479 1997). The model is valid under the following assumptions: (1) constant density of
480 water; (2) no long-term storage change in the reservoir; (3) well-mixed for the
481 epilimnion (Gibson 2002, Gibson et al. 2016, Gibson and Edwards 2002, LaBaugh et
482 al. 1997). The above assumptions are reasonably tenable during the short monitoring

Hydrol. Earth Syst. Sci. Discuss., https://doi.org/10.5194/hess-2018-26
Manuscript under review for journal Hydrol. Earth Syst. Sci.
Discussion started: 12 February 2018

period. The model can be fully expressed as

$$F_{in} + F_{LGD} + F_p = F_E + F_{out} \quad (4)$$

$$F_{in} \times \delta_{in} + F_{LGD} \times \delta_{gw} + F_p \times \delta_p = F_E \times \delta_E + F_{out} \times \delta_L \quad (5)$$

$$F_{in} \times [Cl^-]_{in} + F_{LGD} \times [Cl^-]_{gw} + F_p \times [Cl^-]_p = F_{out} \times [Cl^-]_L \quad (6)$$

where F_{in} [mm d^{-1}] is the surface water inflow to the lake; F_{gw} [mm d^{-1}] is LGD rate. F_p [mm d^{-1}] is the mean daily rainfall rate during the sampling period. F_E [mm d^{-1}] is the lake evaporation. F_{out} [mm d^{-1}] is the lake water outflow via runoff and infiltration into the lake shore aquifer. δ_{in}, δ_{gw},, δ_E and δ_p are the isotopic compositions of surface water inflow, LGD, and evaporative flux, respectively. The values of δ_{in}, δ_{gw},, and δ_p are obtained from field data and the composition of δ_E are cacluated as shown in supplementary information. $[Cl^-]_{in}$, $[Cl^-]_{gw}$, $[Cl^-]_L$ and $[Cl^-]_p$ are the chloride concentrations in the inflow water, porewater, lake water and precipitation, respectively.

The components of the mass balance model can be obtained from the field data of isotopic composition and Cl^- concentrations in different water endmembers. The average ^{18}O composition -13.37 ‰ of riverine inflow water is taken as the value of the input parameter δ_{in}. $\delta^{18}O$ and δ^2H in the groundwater endmember and lake water end member are calculated to be -12.41 ‰ and -87.18 ‰, respectively. $\delta^{18}O$ and δ^2H in the rainfall are measured to be -5.47 ‰ and -24.98 ‰, respectively. With the

Hydrol. Earth Syst. Sci. Discuss., https://doi.org/10.5194/hess-2018-26
Manuscript under review for journal Hydrol. Earth Syst. Sci.
Discussion started: 12 February 2018

measured values of δ_L, h, δ_{in}, and the estimated ε and δ_a, the isotopic composition of δ_E is calculated to be -35.11 ‰, which is in line with the results of alpine and arctic lakes elsewhere (Gibson 2002, Gibson et al. 2016, Gibson and Edwards 2002). The values of $[Cl^-]_{in}$, $[Cl^-]_{gw}$, and $[Cl^-]_L$ are calculated to be 0.91 mg L^{-1}, 1.48 mg L^{-1} and 1.02 mg L^{-1}, respectively. All the parameters used in the model are shown in Table 2.

According to Equations 4-6, the uncertainties of calculations of F_{in}, F_{out} and E are mainly derived from the uncertainty of F_{LGD} and the compositions of Cl^-, δD and $\delta^{18}O$ in different water endmembers as suggested in previous studies (Genereux 1998, Klaus and McDonnell 2013). The compositions of Cl^-, δD and $\delta^{18}O$ in surface water, groundwater endmembers have an uncertainty of 5 %. The uncertainty of δ_E is reasonably assumed to be ≈ 20 % . Thus, considering the uncertainty propagation of all the above parameters, the uncertainties of F_{in}, F_{out} and E would be scaled up to 70-80 % of the final estimates.

4.4 The hydrologic partitioning of the glacial lake

Based on the three endmember model of ^{18}O and Cl^-, the riverine inflow rate was calculated to be 135.6 ± 119.0 mm d^{-1}, and the lake outflow rate is estimated to be 141.5 ± 132.4 mm d^{-1}; the evaporation rate is calculated to be 5.2 ± 4.7 mm d^{-1}. The

summary of the hydrologic partitioning of the lake is shown in Figure 8a. Generally, the proglacial lake is mostly recharged by the riverine inflow from the snowpack or the glacier melting. The groundwater discharge contributes about only 7.0 % of the total water input to the lake, indicating groundwater input does not dominate water input to the proglacial lake. The lake water is mainly lost via surface water outflow and infiltration to the lake shore aquifers. The evaporation constitutes relatively small ratio (≈ 3.5 %) of total water losses. The annual evaporation rate was recorded to be 1429.8 mm (equivalent to 3.92 mm d^{-1}) in 2015 by the Jiuzhi weather station, lower than the obtained evaporation in this study. This may be due to much higher evaporation in August during the monitoring period. The recent review on LGD rate by Rosenberry et al. (2015) suggests that the median of LGD rate in the literatures is 7.4 mm d^{-1} (0.05 mm d^{-1} to 133 mm d^{-1}), which is about 2/3 of LGD rate in this study. This difference may be due to the hydrogeological setting of the lake shore aquifer. This aquifer is formed by grey loam, clayey soil and sand (Lehmkuhl 1998, Schlutz and Lehmkuhl 2009), which is with relatively high permeability. Previous studies have indicated that groundwater forms a key component of proglacial hydrology (Levy et al. 2015). However, there have been limited quantitative studies of groundwater contribution to hydrologic budget of proglacial areas. This study summarizes the groundwater discharge studies over the glacial forefield areas. Brown

et al. (2006) investigated the headwater streams at the proglacial areas of Taillon Glacier in French and found that groundwater contributes 6-10 % of the stream water immediate downwards of the glacier. Using water mass balance model, Hood et al. (2006) shows that groundwater inflow is substantial in the hydrologic partitioning of the proglacial Lake O'Hara in front of Opabin Glacier in Canada and comprised of 30 -74 % of the total inflow. Roy and Hayashi (2008) studied the proglacial lakes of Hungabee lake and Opabin lake at glacier forefield of Opabin Glacier and found that groundwater component is predominant water sources of the lakes and consisted of 35-39 % of the total water input of the lakes. Langston et al. (2013) further investigated a tarn immediate in front of Opabin Glacier and indicated the tarn is predominantly controlled by groundwater inflow/outflow, which consisted of 50-100 % of total tarn volume. Magnusson et al. (2014) studied the streams in the glacier forefield of Dammagletscher, Switzerland and revealed that groundwater contributed only 1-8 % of the total surface runoff. Groundwater contribution in this study is similar to those obtained the mountainous proglacial areas in Europe, but much lower than those obtained in the proglacial areas of polar regions. It is concluded that proglacial lakes/streams in front of mountainous glaciers are mainly recharged by surface runoff from glacier/snowpack melting. This might be due to well-developed stream networks and limited deep groundwater flow (Brown et al. 2006, Einarsdottir

559 et al. 2017, Magnusson et al. 2014). However, proglacial tarns and lakes in the polar
560 areas are predominantly controlled by groundwater discharge, due to less connectivity
561 of surface runoff and high shallow and deep groundwater connectivity (Hood et al.
562 2006, Langston et al. 2013, Roy and Hayashi 2008).

563 4.5 LGD derived nutrient loadings, nutrient budget and ecological implications

564 Compared to extensive studies of SGD derived nutrient loadings in the past decade
565 (Luo and Jiao 2016, Slomp and Van Cappellen 2004), studies of LGD derived nutrient
566 loadings have received limited attention, even given the fact that groundwater in lake
567 shore aquifers is usually concentrated in nutrients (Lewandowski et al. 2015,
568 Rosenberry et al. 2015). Even fewer studies focus on chemical budgets in the
569 proglacial lakes which are often difficult to access for sampling. Groundwater borne
570 DIN and DIP across the sediment-water interface in this study are determined with an
571 equation coupling the advective or LGD-derived, and diffusive solute transport
572 (Hagerthey and Kerfoot 1998, Lerman et al. 1995)

573 $$F_j = -nD_j^m \frac{dC_j}{dx} + v_{gw} C_j \quad (7)$$

574 where $-nD_j^m \frac{dC_j}{dx}$ is the diffusion input and $v_{gw} C_j$ is the LGD derived fluxes, F_j
575 [μM m^{-2} d^{-1}] is the mol flux of nutrient species *j* (representing DIN or DIP). *n* is the
576 sediment porosity. D_j^m is the molecular diffusion coefficient of nutrient species *j*,

Hydrol. Earth Syst. Sci. Discuss., https://doi.org/10.5194/hess-2018-26
Manuscript under review for journal Hydrol. Earth Syst. Sci.
Discussion started: 12 February 2018

577 which is given to be 4.8 x 10^{-5} m^2 d^{-1} for DIP (Quigley and Robbins 1986), and 8.8 x
578 10^{-5} m^2 d^{-1} for DIN (Li and Gregory 1974), respectively. C_j [μM] is the concentration
579 of nutrient species *j*. *x*[m] is the sampling depth. v_{gw} is LGD rate estimated by ^{222}Rn
580 mass balance model and has a value of 10.3 ± 8.2 mm d^{-1}. $\frac{dC_j}{dx}$ is the concentration
581 gradient of nutrient species *j* across the water-sedimentary interface.
582 Substituting the constants and the field data of DIN and DIP in to Equation 6, LGD
583 derived nutrient loadings are calculated to be 954.3 μmol m^{-2} d^{-1} and 3.2 μmol m^{-2} d^{-1}
584 for DIN and DIP, respectively. Riverine inflow brings 1195.0 μmol m^{-2} d^{-1} DIN, 52.9
585 μmol m^{-2} d^{-1} DIP into the lake. Lake water outflow derived nutrient loss is estimated
586 to be 1439.9 μmol m^{-2} d^{-1} and 54.7 μmol m^{-2} d^{-1} for DIN and DIP, respectively.
587 Nutrients in the lake can be also sourced from atmospheric deposit (mostly in form of
588 precipitation). With the nutrient concentrations in the rain water during the monitoring
589 period, the wet deposit is calculated to be 76 μmol m^{-2} d^{-1} and 2.5 μmol m^{-2} d^{-1}, for
590 DIN and DIP, respectively. The loadings of DIN to the lakes are mainly from surface
591 runoff and LGD, which comprised of 42.9 % and 53.7 % of the total DIN loadings..
592 Groundwater derived DIP input, however, constitutes only 6.3 % of the total DIP
593 inputs to the lake, indicating groundwater borne DIP is less contributive to the
594 nutrient budget of the lake compared to DIN. Very recent studies on polar regions
595 have indicated that the glacier/snowpack water is the main N sources to the proglacial

596 lakes (Anderson et al. 2013, Dubnick et al. 2017). However, they do not consider the
597 contribution of groundwater borne N, in spite of the high groundwater connectivity in
598 the proglacial areas (Roy and Hayashi 2008). This study stresses that groundwater
599 borne DIN could be comparable to the surface runoff derived DIN.

600 Based on nutrient results, the lake is considered to be an oligotrophic lake and
601 under phosphate limited condition. Thus, the primary production (PP) is therefore
602 considered to be controlled by the DIP loadings. The sum of DIN and DIP inputs
603 minus the sum of the calculated DIN and DIP outputs leads to surpluses of 785.4
604 μmol m^{-2} d^{-1} and 3.9 μmol m^{-2} d^{-1} for DIN and DIP, respectively. The surpluses are
605 expected to be consumed by the phytoplankton and converted into the PP under the
606 Red Field ratio (C: N: P = 106: 16: 1), leading to a PP of 0.41 mmol C m^{-2} d^{-1}. The
607 nutrient budgets for DIN and DIP are summarized in Figures 8b and 8c. The estimated
608 primary productivity is lower than most temperate eutrophicated and ologotrophic
609 lakes (Cole et al. 1998, Smith 1979), and comparable to some high latitude or altitude
610 lakes (Richerson et al. 1986, Sterner 2010).

611 4.6. Implications, prospective and limitations

612 Mountainous proglacial lakes are readily developed in glacier forefields of QTP and
613 other high mountainous glacial such as Europe Alps and Pamir at central Asian
614 (Heckmann et al. 2016). The proglacial lakes are always trapping system of sediment

and sinks for water and chemical originated from glacier/snowpack melting and groundwater. In analogous to cosmogenic isotopes such as ^{10}Be serving as a tool to quantify the sediment sources, approaches integrating ^{222}Rn and stable isotopes provides both qualitatively and quantitatively evaluations of groundwater contributions and hydrologic partitioning in these remote and untapped lacustrine systems. Thus, it is expected that the multiple aqueous isotopes is considered to be effective tools to investigate the LGD and hydrologic partitioning in other proglacial lakes. This study is mainly limited by the relatively short sampling and monitoring period. As a special hydrologic regime, the lake shore aquifers of the proglacial lakes are experiencing frozen-unfrozen transition seasonally, and the dominant recharge of glacial melting could be fluctuated significantly due to air temperature variation. Therefore, future groundwater and hydrological studies can be extended to longtime sampling and monitoring of stable isotopes and ^{222}Rn in different water endmembers to reveal the seasonally hydrological and hydrogeological dynamics and their impacts on local biogeochemical cycles and ecological systems. Special concerns would be placed on how surface/groundwater interactions and the associated biogeochemical processes in response to the seasonal frozen ground variations and glacier/snowpack melting intensity.

Hydrol. Earth Syst. Sci. Discuss., https://doi.org/10.5194/hess-2018-26
Manuscript under review for journal Hydrol. Earth Syst. Sci.
Discussion started: 12 February 2018

5. Conclusion

A ^{222}Rn continuous monitoring is conducted at Ximen Co Lake, a proglacial lake located at the east QTP. A dynamic ^{222}Rn mass balance model constrained by radium mass balance and water level fluctuation is used to quantify temporal distribution of LGD of the lake. The obtained LGD over the monitoring time ranges from – 23. 7 mm d^{-1} to 80.9 mm d^{-1}, with an average of 10.3 ± 8.2 mm d^{-1}. Thereafter, a three endmember model consisting of the budgets of water, stable isotopes and Cl^- is used to depict the hydrologic partitioning of the lake. Riverine inflow, lake water outflow via surface runoff, and surface evaporation are estimated to be 135.6 mm d^{-1}, 141.5 mm d^{-1} and 5.2 mm d^{-1}, respectively. LGD derived nutrient loading is estimated to be 785.4 μmol m^{-2} d^{-1} and 3.2 μmol m^{-2} d^{-1} for DIN and DIP, respectively. Upon depicting nutrient budget within the lake, the primary productivity is estimated to be 0.41 mol C m^{-2} d^{-1}. This study also implicates that LGD constitutes relatively small portion of the proglacial hydrologic partitioning, however, delivers nearly a half of the nutrient loadings to the proglacial lake.

This study presents the first attempt to quantify LGD and the associated nutrient loadings to the proglacial lake of QTP. To our knowledge, there is almost no study on the groundwater-lake water interaction in the high altitude proglacial lakes in QTP. This study demonstrates that ^{222}Rn based approach can be used to investigate the

groundwater dynamics in the high altitude proglacial lakes. The method is instructional to similar studies in other proglacial lakes in the QTP and elsewhere.

Acknowledgements

This study was supported by a grant from the National Natural Science Foundation of China (NSFC, No.41572208) and the Research Grants Council of Hong Kong Special Administrative Region, China (HKU17304815). The authors thank Mr. Buming Jiang for his kind help in the field works during the campaign and Ergang Lian for his help in stable isotope analysis. The authors thank Jessie Lai for her help in FIA analysis in School of Biological Sciences, HKU. Supporting data are included as in the files of supplementary information 2 and 3; Climatological data are purchased through http://www.weatherdt.com/shop.html; any additional data may be obtained from L.X. (email: xinluo@hku.hk);

References

Åberg, J., Jansson, M. and Jonsson, A. (2010) Importance of water temperature and thermal stratification dynamics for temporal variation of surface water CO_2 in a boreal lake. Journal of Geophysical Research: Biogeosciences (2005–2012) 115(G2).

Andermann, C., Longuevergne, L., Bonnet, S., Crave, A., Davy, P. and Gloaguen, R. (2012) Impact of transient groundwater storage on the discharge of Himalayan rivers. Nature Geoscience 5(2), 127-132.

Anderson, L., Birks, J., Rover, J. and Guldager, N. (2013) Controls on recent Alaskan lake changes identified from water isotopes and remote sensing. Geophysical

676 Research Letters 40(13), 3413-3418.
677 Anderson, N.J., Saros, J.E., Bullard, J.E., Cahoon, S.M., McGowan, S., Bagshaw, E.A.,
678 Barry, C.D., Bindler, R., Burpee, B.T. and Carrivick, J.L. (2017) The Arctic in the
679 Twenty-First Century: Changing Biogeochemical Linkages across a Paraglacial
680 Landscape of Greenland. BioScience 67(2), 118-133.
681 Barry, R.G. (2006) The status of research on glaciers and global glacier recession: a
682 review. Progress in Physical Geography 30(3), 285-306.
683 Batlle-Aguilar, J., Harrington, G.A., Leblanc, M., Welch, C. and Cook, P.G. (2014)
684 Chemistry of groundwater discharge inferred from longitudinal river sampling. Water
685 Resources Research 50(2), 1550-1568.
686 Belanger, T.V., Mikutel, D.F. and Churchill, P.A. (1985) Groundwater seepage nutrient
687 loading in a Florida Lake. Water Research 19(6), 773-781.
688 Blume, T., Krause, S., Meinikmann, K. and Lewandowski, J. (2013) Upscaling lacustrine
689 groundwater discharge rates by fiber-optic distributed temperature sensing. Water
690 Resources Research 49(12), 7929-7944.
691 Böhner, J. (1996) Säkulare Klimaschwankungen und rezente Klimatrends Zentral-und
692 Hochasiens, Goltze.
693 Böhner, J. (2006) General climatic controls and topoclimatic variations in Central and
694 High Asia. Boreas 35(2), 279-295.
695 Bolch, T., Kulkarni, A., Kääb, A., Huggel, C., Paul, F., Cogley, J.G., Frey, H., Kargel, J.S.,
696 Fujita, K., Scheel, M., Bajracharya, S. and Stoffel, M. (2012) The State and Fate of
697 Himalayan Glaciers. Science 336(6079), 310-314.
698 Brown, L.E., Hannah, D.M., Milner, A.M., Soulsby, C., Hodson, A.J. and Brewer, M.J.
699 (2006) Water source dynamics in a glacierized alpine river basin (Taillon-Gabiétous,
700 French Pyrénées). Water Resources Research 42(8).
701 Burnett, W.C., Peterson, R.N., Santos, I.R. and Hicks, R.W. (2010) Use of automated
702 radon measurements for rapid assessment of groundwater flow into Florida streams.
703 Journal of Hydrology 380(3), 298-304.
704 Callegary, J.B., Kikuchi, C.P., Koch, J.C., Lilly, M.R. and Leake, S.A. (2013) Review:
705 Groundwater in Alaska (USA). Hydrogeology Journal 21(1), 25-39.
706 Cole, J., Nina, J. and Caraco, F. (1998) Atmospheric exchange of carbon dioxide in a
707 low-wind oligotrophic lake measured by the addition of SF_6. Limnology and
708 Oceanography 43, 647-656.
709 Cook, P., Lamontagne, S., Berhane, D. and Clark, J. (2006) Quantifying groundwater
710 discharge to Cockburn River, southeastern Australia, using dissolved gas tracers ^{222}Rn
711 and SF_6. Water Resources Research 42(10).
712 Cook, P.G., Favreau, G., Dighton, J.C. and Tickell, S. (2003) Determining natural
713 groundwater influx to a tropical river using radon, chlorofluorocarbons and ionic

714 environmental tracers. Journal of Hydrology 277(1–2), 74-88.
715 Corbett, D.R., Burnett, W.C., Cable, P.H. and Clark, S.B. (1997) Radon tracing of
716 groundwater input into Par Pond, Savannah River site. Journal of Hydrology 203(1),
717 209-227.
718 Cui, X., Ren, J., Qin, X., Sun, W., Yu, G., Wang, Z. and Liu, W. (2014) Chemical
719 characteristics and environmental records of a snow-pit at the Glacier No. 12 in the
720 Laohugou Valley, Qilian Mountains. Journal of Earth Science 25(2), 379-385.
721 Dansgaard, W. (1964) Stable isotopes in precipitation. Tellus A 16(4).
722 Dimova, N., Paytan, A., Kessler, J.D., Sparrow, K., Garcia-Tigreros Kodovska, F., Lecher,
723 A.L., Murray, J. and Tulaczyk, S.M. (2015) The current magnitude and mechanisms of
724 groundwater discharge in the Arctic: a case study from Alaska. Environmental Science
725 & Technology 49(20), 12036-12043.
726 Dimova, N.T. and Burnett, W.C. (2011) Evaluation of groundwater discharge into small
727 lakes based on the temporal distribution of radon-222. Limnol. Oceanogr 56(2),
728 486-494.
729 Dimova, N.T., Burnett, W.C., Chanton, J.P. and Corbett, J.E. (2013) Application of
730 radon-222 to investigate groundwater discharge into small shallow lakes. Journal of
731 Hydrology.
732 Dubnick, A., Wadham, J., Tranter, M., Sharp, M., Orwin, J., Barker, J., Bagshaw, E. and
733 Fitzsimons, S. (2017) Trickle or treat: The dynamics of nutrient export from polar
734 glaciers. Hydrological Processes 31(9), 1776-1789.
735 Einarsdottir, K., Wallin, M.B. and Sobek, S. (2017) High terrestrial carbon load via
736 groundwater to a boreal lake dominated by surface water inflow. Journal of
737 Geophysical Research: Biogeosciences, 122(1), 15-29.
738 Farinotti, D., Longuevergne, L., Moholdt, G., Duethmann, D., Molg, T., Bolch, T.,
739 Vorogushyn, S. and Guntner, A. (2015) Substantial glacier mass loss in the Tien Shan
740 over the past 50 years. Nature Geosci 8(9), 716-722.
741 Gat, J. (1995) Physics and chemistry of lakes, pp. 139-165, Springer.
742 Gat, J. (1996) Oxygen and hydrogen isotopes in the hydrologic cycle. Annual Review
743 of Earth and Planetary Sciences 24(1), 225-262.
744 Genereux, D. (1998) Quantifying uncertainty in tracer-based hydrograph separations.
745 Water Resources Research 34(4), 915-919.
746 Gibson, J., Edwards, T., Bursey, G. and Prowse, T. (1993) Estimating evaporation using
747 stable isotopes: quantitative results and sensitivity analysis for. Nordic Hydrology 24,
748 79-94.
749 Gibson, J.J. (2002) Short-term evaporation and water budget comparisons in shallow
750 Arctic lakes using non-steady isotope mass balance. Journal of Hydrology 264(1),
751 242-261.

752 Gibson, J.J., Birks, S.J. and Yi, Y. (2016) Stable isotope mass balance of lakes: a
753 contemporary perspective. Quaternary Science Reviews 131, Part B, 316-328.
754 Gibson, J.J. and Edwards, T.W.D. (2002) Regional water balance trends and
755 evaporation-transpiration partitioning from a stable isotope survey of lakes in
756 northern Canada. Global Biogeochemical Cycles 16(2), 10-11-10-14.
757 Gilfedder, B., Frei, S., Hofmann, H. and Cartwright, I. (2015) Groundwater discharge
758 to wetlands driven by storm and flood events: Quantification using continuous
759 Radon-222 and electrical conductivity measurements and dynamic mass-balance
760 modelling. Geochimica Et Cosmochimica Acta 165, 161-177.
761 Gonfiantini, R. (1986) Environmental isotopes in lake studies. Handbook of
762 environmental isotope geochemistry 2, 113-168.
763 Hagerthey, S.E. and Kerfoot, W.C. (1998) Groundwater flow influences the biomass
764 and nutrient ratios of epibenthic algae in a north temperate seepage lake. Limnology
765 and Oceanography 43(6), 1227-1242.
766 Harris, C., Arenson, L.U., Christiansen, H.H., Etzelmüller, B., Frauenfelder, R., Gruber,
767 S., Haeberli, W., Hauck, C., Hölzle, M. and Humlum, O. (2009) Permafrost and climate
768 in Europe: Monitoring and modelling thermal, geomorphological and geotechnical
769 responses. Earth-Science Reviews 92(3), 117-171.
770 Hasler, C.T., Midway, S.R., Jeffrey, J.D., Tix, J.A., Sullivan, C. and Suski, C.D. (2016)
771 Exposure to elevated pCO2 alters post-treatment diel movement patterns of
772 largemouth bass over short time scales. Freshwater Biology 61(9), 1590-1600.
773 Hawkings, J., Wadham, J., Tranter, M., Telling, J., Bagshaw, E., Beaton, A., Simmons,
774 S.L., Chandler, D., Tedstone, A. and Nienow, P. (2016) The Greenland Ice Sheet as a
775 hot spot of phosphorus weathering and export in the Arctic. Global Biogeochemical
776 Cycles.
777 Heckmann, T., McColl, S. and Morche, D. (2016) Retreating ice: research in pro-glacial
778 areas matters. Earth Surface Processes and Landforms, 41(2), 271-276.
779 Hodson, A. (2007) Phosphorus in glacial meltwaters. Glacier Science and
780 Environmental Change, 81-82.
781 Hodson, A., Mumford, P., Kohler, J. and Wynn, P.M. (2005) The High Arctic glacial
782 ecosystem: new insights from nutrient budgets. Biogeochemistry 72(2), 233-256.
783 Hood, J.L., Roy, J.W. and Hayashi, M. (2006) Importance of groundwater in the water
784 balance of an alpine headwater lake. Geophysical Research Letters 33(13).
785 Hren, M.T., Bookhagen, B., Blisniuk, P.M., Booth, A.L. and Chamberlain, C.P. (2009)
786 $\delta^{18}O$ and δD of streamwaters across the Himalaya and Tibetan Plateau: Implications
787 for moisture sources and paleoelevation reconstructions. Earth and Planetary
788 Science Letters 288(1), 20-32.
789 Hudson, J.J., Taylor, W.D. and Schindler, D.W. (2000) Phosphate concentrations in

790 lakes. Nature 406(6791), 54-56.
791 Johannes, R.E. (1980) The Ecological Significance of the Submarine Discharge of
792 Groundwater. Marine Ecology-Progress Series 3(4), 365-373.
793 Kim, G., Burnett, W.C., Dulaiova, H., Swarzenski, P.W. and Moore, W.S. (2001)
794 Measurement of Ra-224 and Ra-226 activities in natural waters using a radon-in-air
795 monitor. Environmental Science & Technology 35(23), 4680-4683.
796 Klaus, J. and McDonnell, J. (2013) Hydrograph separation using stable isotopes:
797 Review and evaluation. Journal of Hydrology 505, 47-64.
798 Kluge, T., Ilmberger, J., Rohden, C.v. and Aeschbach-Hertig, W. (2007) Tracing and
799 quantifying groundwater inflow into lakes using a simple method for radon-222
800 analysis. Hydrology and Earth System Sciences 11(5), 1621-1631.
801 Kluge, T., von Rohden, C., Sonntag, P., Lorenz, S., Wieser, M., Aeschbach-Hertig, W.
802 and Ilmberger, J. (2012) Localising and quantifying groundwater inflow into lakes
803 using high-precision ^{222}Rn profiles. Journal of Hydrology 450, 70-81.
804 Kraemer, T.F. (2005) Radium isotopes in Cayuga Lake, New York: Indicators of inflow
805 and mixing processes. Limnology and Oceanography 50(1), 158-168.
806 LaBaugh, J.W., Rosenberry, D.O. and Winter, T.C. (1995) Groundwater contribution to
807 the water and chemical budgets of Williams Lake, Minnesota, 1980-1991. Canadian
808 Journal of Fisheries and Aquatic Sciences 52(4), 754-767.
809 LaBaugh, J.W., Winter, T.C., Rosenberry, D.O., Schuster, P.F., Reddy, M.M. and Aiken,
810 G.R. (1997) Hydrological and chemical estimates of the water balance of a closed-
811 basin lake in north central Minnesota. Water Resources Research 33(12), 2799-2812.
812 Langston, G., Hayashi, M. and Roy, J.W. (2013) Quantifying groundwater-surface
813 water interactions in a proglacial moraine using heat and solute tracers. Water
814 Resources Research 49(9), 5411-5426.
815 Lazar, B., Weinstein, Y., Paytan, A., Magal, E., Bruce, D. and Kolodny, Y. (2008) Ra and
816 Th adsorption coefficients in lakes—Lake Kinneret (Sea of Galilee) "natural
817 experiment". Geochimica Et Cosmochimica Acta 72(14), 3446-3459.
818 Lecher, A.L., Kessler, J., Sparrow, K., Garcia-Tigreros Kodovska, F., Dimova, N., Murray,
819 J., Tulaczyk, S. and Paytan, A. (2015) Methane transport through submarine
820 groundwater discharge to the North Pacific and Arctic Ocean at two Alaskan sites.
821 Limnology and Oceanography, 61(S1).
822 Lee, C.M., Jiao, J.J., Luo, X. and Moore, W.S. (2012) Estimation of submarine
823 groundwater discharge and associated nutrient fluxes in Tolo Harbour, Hong Kong.
824 Science of the Total Environment 433, 427-433.
825 Lee, D.R. (1977) A device for measuring seepage flux in lakes and estuaries.
826 Limnology and Oceanography 22(1), 140-147.
827 Lee, D.R., Cherry, J.A. and Pickens, J.F. (1980) Groundwater transport of a salt tracer

828 through a sandy lakebed. Limnology and Oceanography 25(1), 45-61.
829 Lehmkuhl, F. (1998) Extent and spatial distribution of Pleistocene glaciations in
830 eastern Tibet. Quaternary International 45–46, 123-134.
831 Lemieux, J.M., Sudicky, E.A., Peltier, W.R. and Tarasov, L. (2008a) Dynamics of
832 groundwater recharge and seepage over the Canadian landscape during the
833 Wisconsinian glaciation. Journal of Geophysical Research: Earth Surface (2003–2012)
834 113(F1).
835 Lemieux, J.M., Sudicky, E.A., Peltier, W.R. and Tarasov, L. (2008b) Simulating the
836 impact of glaciations on continental groundwater flow systems: 1. Relevant processes
837 and model formulation. Journal of Geophysical Research: Earth Surface 113(F3).
838 Lemieux, J.M., Sudicky, E.A., Peltier, W.R. and Tarasov, L. (2008c) Simulating the
839 impact of glaciations on continental groundwater flow systems: 2. Model application
840 to the Wisconsinian glaciation over the Canadian landscape. Journal of Geophysical
841 Research: Earth Surface (2003–2012) 113(F3).
842 Lerman, A., Imboden, D. and Gat, J. (1995) Physics and chemistry of lakes. New York.
843 Levy, A., Robinson, Z., Krause, S., Waller, R. and Weatherill, J. (2015) Long-term
844 variability of proglacial groundwater-fed hydrological systems in an area of glacier
845 retreat, Skeiðarársandur, Iceland. Earth Surface Processes and Landforms 40(7),
846 981-994.
847 Lewandowski, J., Meinikmann, K., Nützmann, G. and Rosenberry, D.O. (2015)
848 Groundwater – the disregarded component in lake water and nutrient budgets. Part
849 2: effects of groundwater on nutrients. Hydrological Processes 29(13), 2922-2955.
850 Lewandowski, J., Meinikmann, K., Ruhtz, T., Pöschke, F. and Kirillin, G. (2013)
851 Localization of lacustrine groundwater discharge (LGD) by airborne measurement of
852 thermal infrared radiation. Remote Sensing of Environment 138, 119-125.
853 Li, Y.H. and Gregory, S. (1974) Diffusion of Ions in Sea-Water and in Deep-Sea
854 Sediments. Geochimica Et Cosmochimica Acta 38(5), 703-714.
855 Liu, C., Liu, J., Wang, X.S. and Zheng, C. (2015) Analysis of groundwater–lake
856 interaction by distributed temperature sensing in Badain Jaran Desert, Northwest
857 China. Hydrological Processes, 30(9), 1330-1341.
858 Liu, Y., Yao, T., Jiao, N., Tian, L., Hu, A., Yu, W. and Li, S. (2011) Microbial diversity in
859 the snow, a moraine lake and a stream in Himalayan glacier. Extremophiles 15(3),
860 411-421.
861 Luo, X. and Jiao, J.J. (2016) Submarine groundwater discharge and nutrient loadings
862 in Tolo Harbor, Hong Kong using multiple geotracer-based models, and their
863 implications of red tide outbreaks. Water Research 102, 11-31.
864 Luo, X., Jiao, J.J., Moore, W. and Lee, C.M. (2014) Submarine groundwater discharge
865 estimation in an urbanized embayment in Hong Kong via short-lived radium isotopes

and its implication of nutrient loadings and primary production. Marine Pollution Bulletin 82(1), 144-154.

Luo, X., Jiao, J.J., Wang, X.-s. and Liu, K. (2016) Temporal ^{222}Rn distributions to reveal groundwater discharge into desert lakes: implication of water balance in the Badain Jaran Desert, China. Journal of Hydrology 534, 87-103.

MacIntyre, S., Wannikhof, R., Chanton, J.P., Matson, P.A. and Hariss, R.C. (1995) Biogenic Trace Gases: Measuring Emissions from Soil and Water.

Magnusson, J., Kobierska, F., Huxol, S., Hayashi, M., Jonas, T. and Kirchner, J.W. (2014) Melt water driven stream and groundwater stage fluctuations on a glacier forefield (Dammagletscher, Switzerland). Hydrological Processes 28(3), 823-836.

Moore, W.S. (1976) Sampling radium-228 in the deep ocean. Deep Sea Res. 23, 647-651.

Nakayama, T. and Watanabe, M. (2008) Missing role of groundwater in water and nutrient cycles in the shallow eutrophic Lake Kasumigaura, Japan. Hydrological Processes 22(8), 1150-1172.

Paytan, A., Lecher, A.L., Dimova, N., Sparrow, K.J., Kodovska, F.G.-T., Murray, J., Tulaczyk, S. and Kessler, J.D. (2015) Methane transport from the active layer to lakes in the Arctic using Toolik Lake, Alaska, as a case study. Proceedings of the National Academy of Sciences 112(12), 3636-3640.

Quigley, M.A. and Robbins, J.A. (1986) Phosphorus release processes in nearshore southern Lake Michigan. Canadian Journal of Fisheries and Aquatic Sciences 43(6), 1201-1207.

Ren, W., Yao, T., Xie, S. and He, Y. (2017) Controls on the stable isotopes in precipitation and surface waters across the southeastern Tibetan Plateau. Journal of Hydrology 545, 276-287.

Ren, W., Yao, T., Yang, X. and Joswiak, D.R. (2013) Implications of variations in $\delta^{18}O$ and δD in precipitation at Madoi in the eastern Tibetan Plateau. Quaternary International 313–314, 56-61.

Richerson, P.J., Neale, P.J., Wurtsbaugh, W., René Alfaro, T. and Vincent, W. (1986) Patterns of temporal variation in Lake Titicaca. A high altitude tropical lake. I. Background, physical and chemical processes, and primary production. Hydrobiologia 138(1), 205-220.

Rosenberry, D.O., Lewandowski, J., Meinikmann, K. and Nützmann, G. (2015) Groundwater-the disregarded component in lake water and nutrient budgets. Part 1: effects of groundwater on hydrology. Hydrological Processes 29(13), 2895-2921.

Roy, J.W. and Hayashi, M. (2008) Groundwater exchange with two small alpine lakes in the Canadian Rockies. Hydrological Processes 22(15), 2838-2846.

Schafran, G.C. and Driscoll, C.T. (1993) Flow path-composition relationships for

groundwater entering an acidic lake. Water Resources Research 29(1), 145-154.
Scheidegger, J.M. and Bense, V.F. (2014) Impacts of glacially recharged groundwater flow systems on talik evolution. Journal of Geophysical Research: Earth Surface 119(4), 758-778.
Schlutz, F. and Lehmkuhl, F. (2009) Holocene climatic change and the nomadic Anthropocene in Eastern Tibet: palynological and geomorphological results from the Nianbaoyeze Mountains. Quaternary Science Reviews 28(15-16), 1449-1471.
Schmidt, A., Gibson, J.J., Santos, I.R., Schubert, M., Tattrie, K. and Weiss, H. (2010) The contribution of groundwater discharge to the overall water budget of two typical Boreal lakes in Alberta/Canada estimated from a radon mass balance. Hydrology and Earth System Sciences 14(1), 79-89.
Sebok, E., Duque, C., Kazmierczak, J., Engesgaard, P., Nilsson, B., Karan, S. and Frandsen, M. (2013) High-resolution distributed temperature sensing to detect seasonal groundwater discharge into Lake Væng, Denmark. Water Resources Research 49(9), 5355-5368.
Shaw, R.D. and Prepas, E.E. (1990) Groundwater-lake interactions: I. Accuracy of seepage meter estimates of lake seepage. Journal of Hydrology 119(1–4), 105-120.
Slaymaker, O. (2011) Criteria to distinguish between periglacial, proglacial and paraglacial environments. Quaestiones Geographicae 30(1), 85-94.
Slomp, C.P. and Van Cappellen, P. (2004) Nutrient inputs to the coastal ocean through submarine groundwater discharge: controls and potential impact. Journal of Hydrology 295(1-4), 64-86.
Smerdon, B., Mendoza, C. and Devito, K. (2007) Simulations of fully coupled lake-groundwater exchange in a subhumid climate with an integrated hydrologic model. Water Resources Research 43(1).
Smith, V.H. (1979) Nutrient dependence of primary productivity in lakes. Limnology and Oceanography 24(6), 1051-1064.
Sterner, R.W. (2010) In situ-measured primary production in Lake Superior. Journal of Great Lakes Research 36(1), 139-149.
Stets, E.G., Winter, T.C., Rosenberry, D.O. and Striegl, R.G. (2010) Quantification of surface water and groundwater flows to open- and closed-basin lakes in a headwaters watershed using a descriptive oxygen stable isotope model. Water Resources Research 46(3).
Tockner, K., Malard, F., Uehlinger, U. and Ward, J. (2002) Nutrients and organic matter in a glacial river-floodplain system (Val Roseg, Switzerland). Limnology and Oceanography 47(1), 266-277.
Valiela, I., Teal, J.M., Volkmann, S., Shafer, D. and Carpenter, E.J. (1978) Nutrient and Particulate Fluxes in a Salt-Marsh Ecosystem - Tidal Exchanges and Inputs by

942 Precipitation and Groundwater. Limnology and Oceanography 23(4), 798-812.
943 Wang, C., Dong, Z., Qin, X., Zhang, J., Du, W. and Wu, J. (2016a) Glacier meltwater
944 runoff process analysis using δD and $\delta^{18}O$ isotope and chemistry at the remote
945 Laohugou glacier basin in western Qilian Mountains, China. Journal of Geographical
946 Sciences 26(6), 722-734.
947 Wang, J., Zhu, L., Wang, Y., Ju, J., Xie, M. and Daut, G. (2010) Comparisons between
948 the chemical compositions of lake water, inflowing river water, and lake sediment in
949 Nam Co, central Tibetan Plateau, China and their controlling mechanisms. Journal of
950 Great Lakes Research 36(4), 587-595.
951 Wang, R., Liu, Z., Jiang, L., Yao, Z., Wang, J. and Ju, J. (2016b) Comparison of surface
952 water chemistry and weathering effects of two lake basins in the Changtang Nature
953 Reserve, China. Journal of Environmental Sciences 41, 183-194.
954 Wang, S. (1997) Frozen ground and environment in the Zoige Plateau and its
955 surrounding mountains (In Chinese with English abstract). Journal of Glaciology and
956 Geocryology 19(1), 39-46.
957 Warner, N.R., Christie, C.A., Jackson, R.B. and Vengosh, A. (2013) Impacts of shale gas
958 wastewater disposal on water quality in western Pennsylvania. Environmental
959 Science & Technology 47(20), 11849-11857.
960 Weynell, M., Wiechert, U. and Zhang, C. (2016) Chemical and isotopic (O, H, C)
961 composition of surface waters in the catchment of Lake Donggi Cona (NW China) and
962 implications for paleoenvironmental reconstructions. Chemical Geology 435, 92-107.
963 White, D., Lapworth, D.J., Stuart, M.E. and Williams, P.J. (2016) Hydrochemical
964 profiles in urban groundwater systems: New insights into contaminant sources and
965 pathways in the subsurface from legacy and emerging contaminants. Science of the
966 Total Environment 562, 962-973.
967 Wilson, J. and Rocha, C. (2016) A combined remote sensing and multi-tracer
968 approach for localising and assessing groundwater-lake interactions. International
969 Journal of Applied Earth Observation and Geoinformation 44, 195-204.
970 Winter, T.C. (1999) Relation of streams, lakes, and wetlands to groundwater flow
971 systems. Hydrogeology Journal 7(1), 28-45.
972 Wischnewski, J., Herzschuh, U., Rühland, K.M., Bräuning, A., Mischke, S., Smol, J.P.
973 and Wang, L. (2014) Recent ecological responses to climate variability and human
974 impacts in the Nianbaoyeze Mountains (eastern Tibetan Plateau) inferred from
975 pollen, diatom and tree-ring data. Journal of Paleolimnology 51(2), 287-302.
976 Xin, W., Yongjian, D., Shiyin, L., Lianghong, J., Kunpeng, W., Zongli, J. and Wanqin, G.
977 (2013) Changes of glacial lakes and implications in Tian Shan, central Asia, based on
978 remote sensing data from 1990 to 2010. Environmental Research Letters 8(4),
979 044052.

980 Yao, T., Thompson, L., Yang, W., Yu, W., Gao, Y., Guo, X., Yang, X., Duan, K., Zhao, H.,
981 Xu, B., Pu, J., Lu, A., Xiang, Y., Kattel, D.B. and Joswiak, D. (2012) Different glacier
982 status with atmospheric circulations in Tibetan Plateau and surroundings. Nature
983 Clim. Change 2(9), 663-667.
984 Yao, Z., Wang, R., Liu, Z., Wu, S. and Jiang, L. (2015) Spatial-temporal patterns of
985 major ion chemistry and its controlling factors in the Manasarovar Basin, Tibet.
986 Journal of Geographical Sciences 25(6), 687-700.
987 Yuan, H., Liu, E., Shen, J., Zhou, H., Geng, Q. and An, S. (2014) Characteristics and
988 origins of heavy metals in sediments from Ximen Co Lake during summer monsoon
989 season, a deep lake on the eastern Tibetan Plateau. Journal of Geochemical
990 Exploration 136, 76-83.
991 Zhang, C. and Mischke, S. (2009) A Lateglacial and Holocene lake record from the
992 Nianbaoyeze Mountains and inferences of lake, glacier and climate evolution on the
993 eastern Tibetan Plateau. Quaternary Science Reviews 28(19), 1970-1983.
994 Zlotnik, V.A., Olaguera, F. and Ong, J.B. (2009) An approach to assessment of flow
995 regimes of groundwater-dominated lakes in arid environments. Journal of Hydrology
996 371(1), 22-30.
997 Zlotnik, V.A., Robinson, N.I. and Simmons, C.T. (2010) Salinity dynamics of discharge
998 lakes in dune environments: Conceptual model. Water Resources Research 46(11).
999 Zongxing, L., Qi, F., Wei, L., Tingting, W., Xiaoyan, G., Zongjie, L., Yan, G., Yanhui, P.,
1000 Rui, G. and Bing, J. (2015) The stable isotope evolution in Shiyi glacier system during
1001 the ablation period in the north of Tibetan Plateau, China. Quaternary International
1002 380, 262-271.

1003

1004

1005

1006 **Figure captions**

1007

1008 **Figure 1** The geological and topographic map of the Yellow River Source Region,
1009 Nianbaoyeze glacial mountains (**a**), and the sampling settings of the Ximen Co Lake
1010 (**b**), with the bathymetry map of the lake (**d**). (**c**) Photograph of the Ximen Co Lake
1011 and the surrounding geomorphic settings looking northeast direction on 22 Aug 2015,
1012 showing the late-laying snowpack in the U-shaped valleys of the north part of
1013 Nianbaoyeze MT.

1014

Figure 2 The climatological parameters (wind speed, air temperature, and precipitation) in the Aug, 2015 recorded from Jiuzhi weather station.

Figure 3 The temporal distributions of ^{222}Rn (**a**), water temperature (**b**), water level fluctuation recorded by the divers (**c**), and hourly wind speed and air temperature recorded in Jiuzhi weather station (**d**).

Figure 4 The cross plots of Cl^- versus Na^+ (**a**), SO_4^{2-} versus Cl^- (**b**), Ca^{2+} versus Cl^- (**c**); The relations of ^2H versus ^{18}O (**d**), Cl^- versus ^2H (**e**), and Cl^- versus ^{18}O (**f**).

Figure 5 Cross plots of ^{222}Rn versus DIN (**a**) and DIP (**b**).

Figure 6 The conceptual model of ^{222}Rn transient model (**a**), and three endmember model (**b**).

Figure 7 The results of the final LGD derived from ^{222}Rn transient model.

Figure 8 The hydrologic partition of the proglacial lake of Ximen CO (**a**), and the budgets of DIN (**b**) and DIP (**c**).

Hydrol. Earth Syst. Sci. Discuss., https://doi.org/10.5194/hess-2018-26
Manuscript under review for journal Hydrol. Earth Syst. Sci.
Discussion started: 12 February 2018

1044 Figure 1

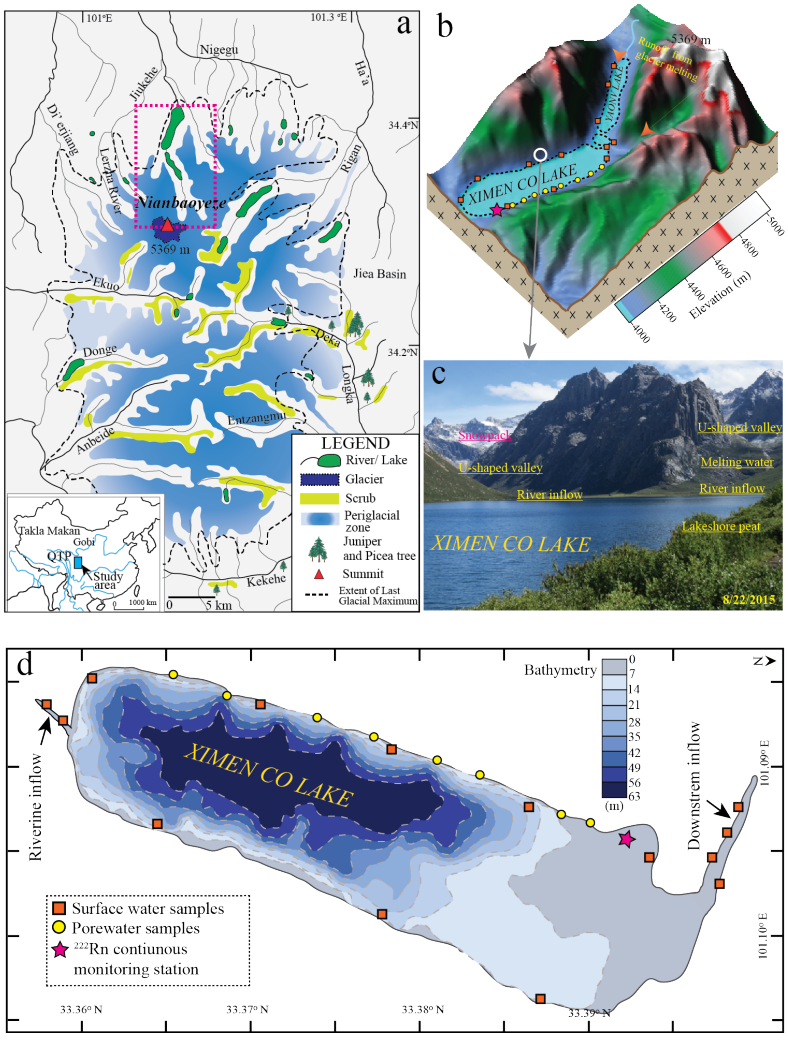

1045

1046

1047

1048

1049

Hydrol. Earth Syst. Sci. Discuss., https://doi.org/10.5194/hess-2018-26
Manuscript under review for journal Hydrol. Earth Syst. Sci.
Discussion started: 12 February 2018

1050 Figure 2

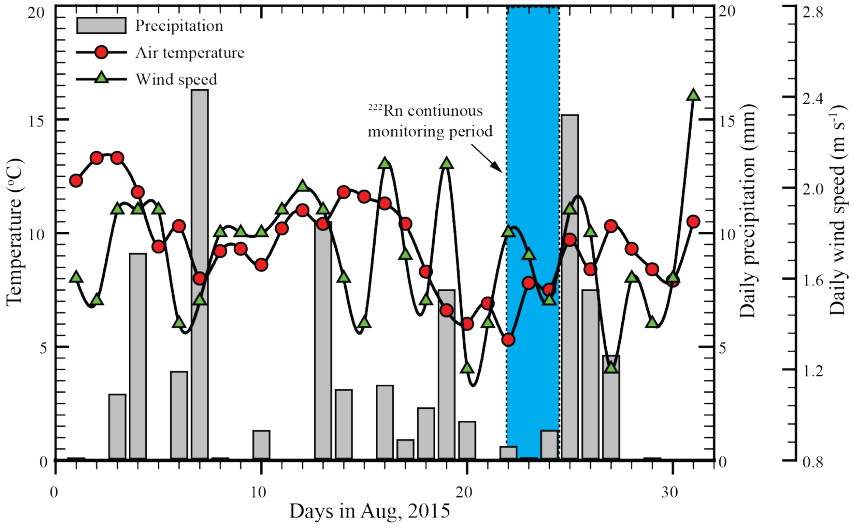

1051

1052

1053

1054

1055

1056

1057

1058

1059

1060

1061

1062

Hydrol. Earth Syst. Sci. Discuss., https://doi.org/10.5194/hess-2018-26
Manuscript under review for journal Hydrol. Earth Syst. Sci.
Discussion started: 12 February 2018

1063 Figure 3

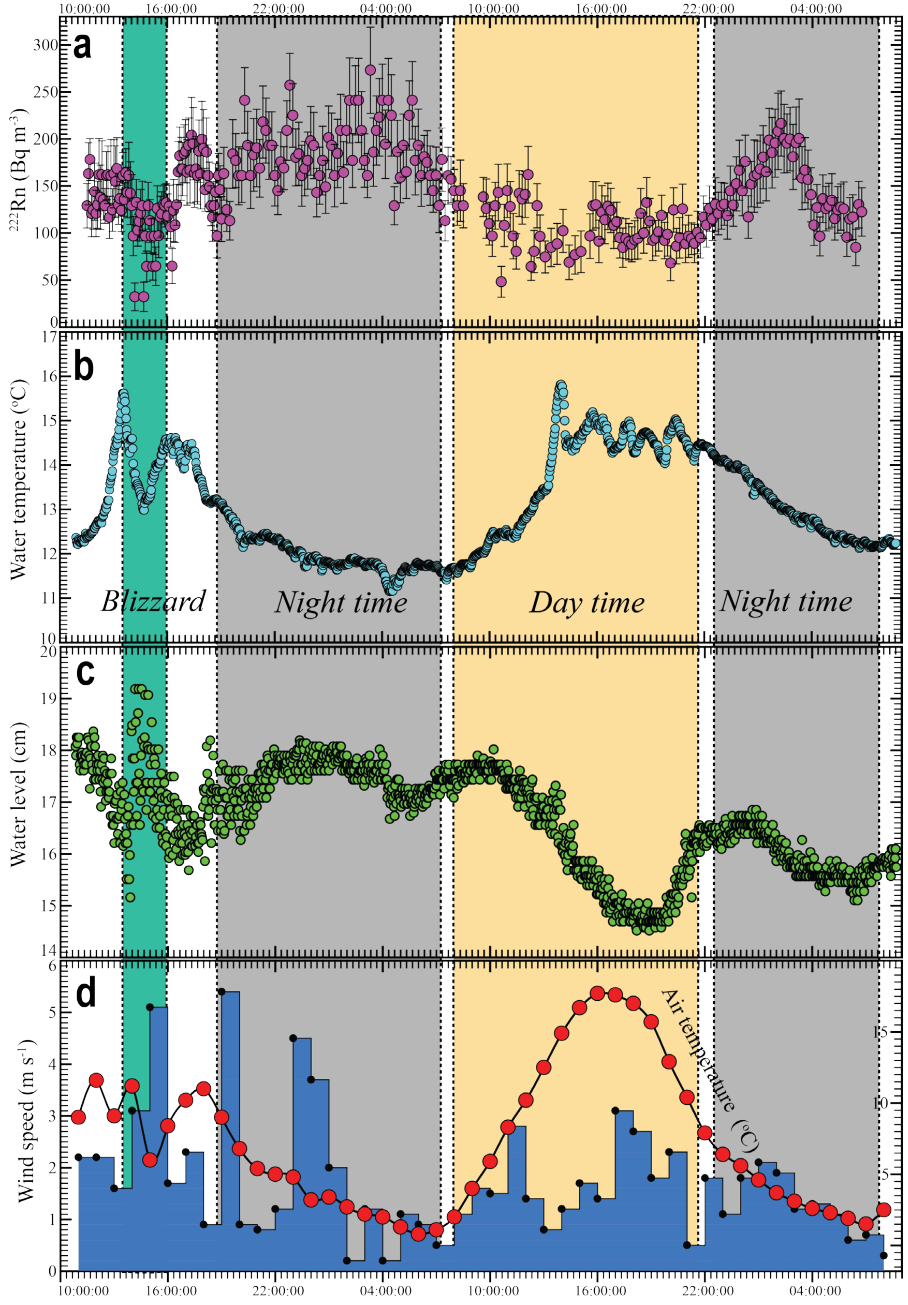

1064

1065

Hydrol. Earth Syst. Sci. Discuss., https://doi.org/10.5194/hess-2018-26
Manuscript under review for journal Hydrol. Earth Syst. Sci.
Discussion started: 12 February 2018

Hydrology and Earth System Sciences
Discussions

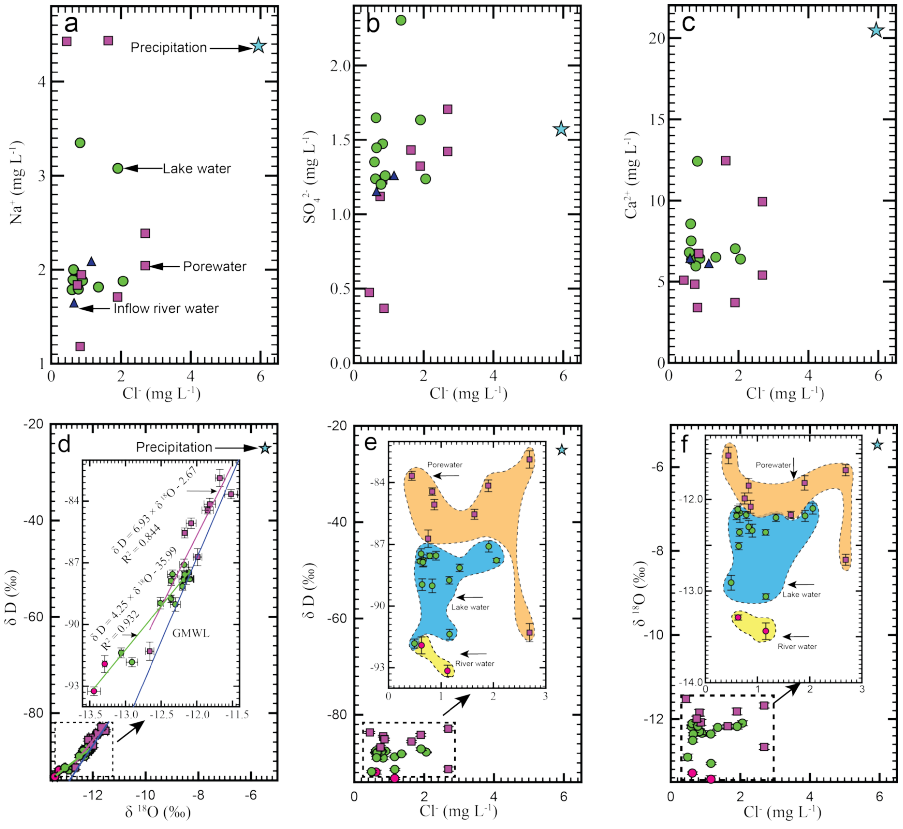

1066

1067

1068

1069

1070

1071

1072

1073

1074

Hydrol. Earth Syst. Sci. Discuss., https://doi.org/10.5194/hess-2018-26
Manuscript under review for journal Hydrol. Earth Syst. Sci.
Discussion started: 12 February 2018

1075 Figure 6

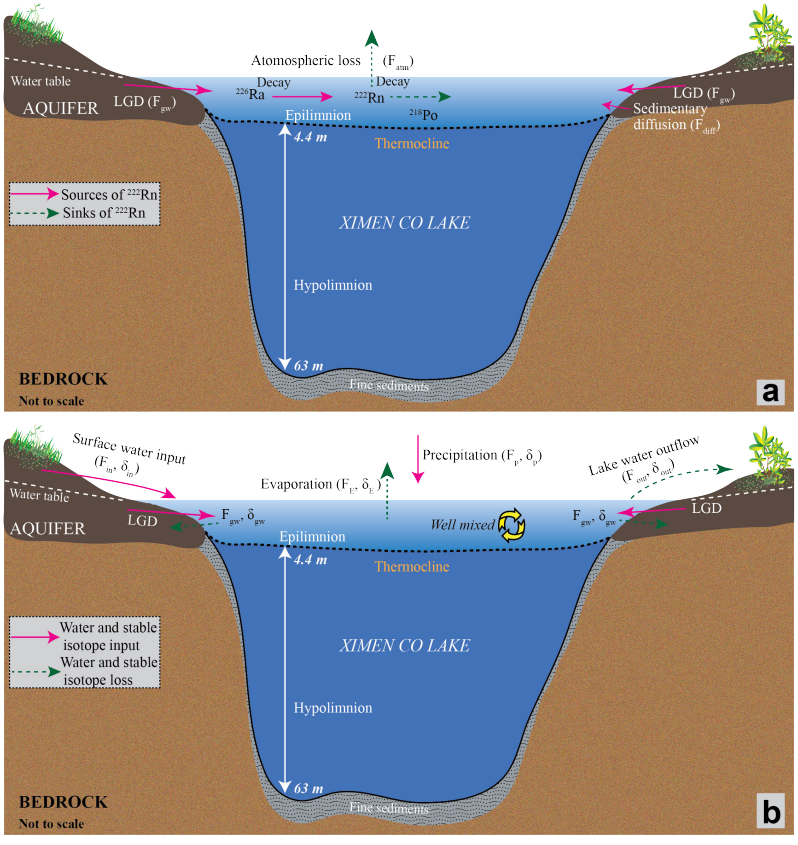

1076

1077

1078

1079

1080

1081

1082

1083

Hydrol. Earth Syst. Sci. Discuss., https://doi.org/10.5194/hess-2018-26
Manuscript under review for journal Hydrol. Earth Syst. Sci.
Discussion started: 12 February 2018

1084 Figure 7

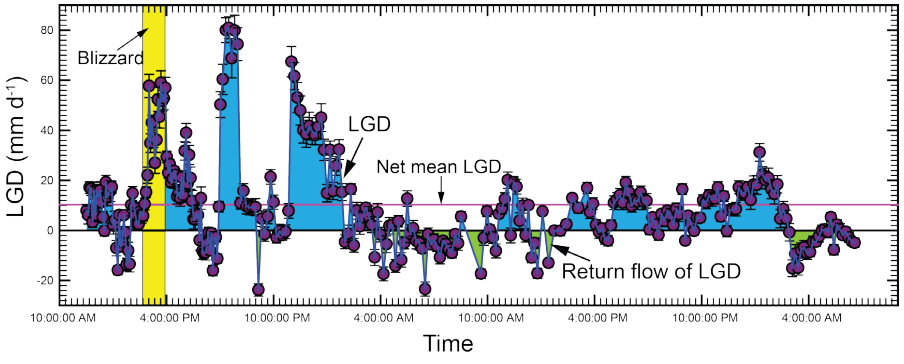

1085

1086

1087

1088

1089

1090

1091

1092

1093

1094

1095

1096

1097

1098

Hydrol. Earth Syst. Sci. Discuss., https://doi.org/10.5194/hess-2018-26
Manuscript under review for journal Hydrol. Earth Syst. Sci.
Discussion started: 12 February 2018

1099 Figure 8

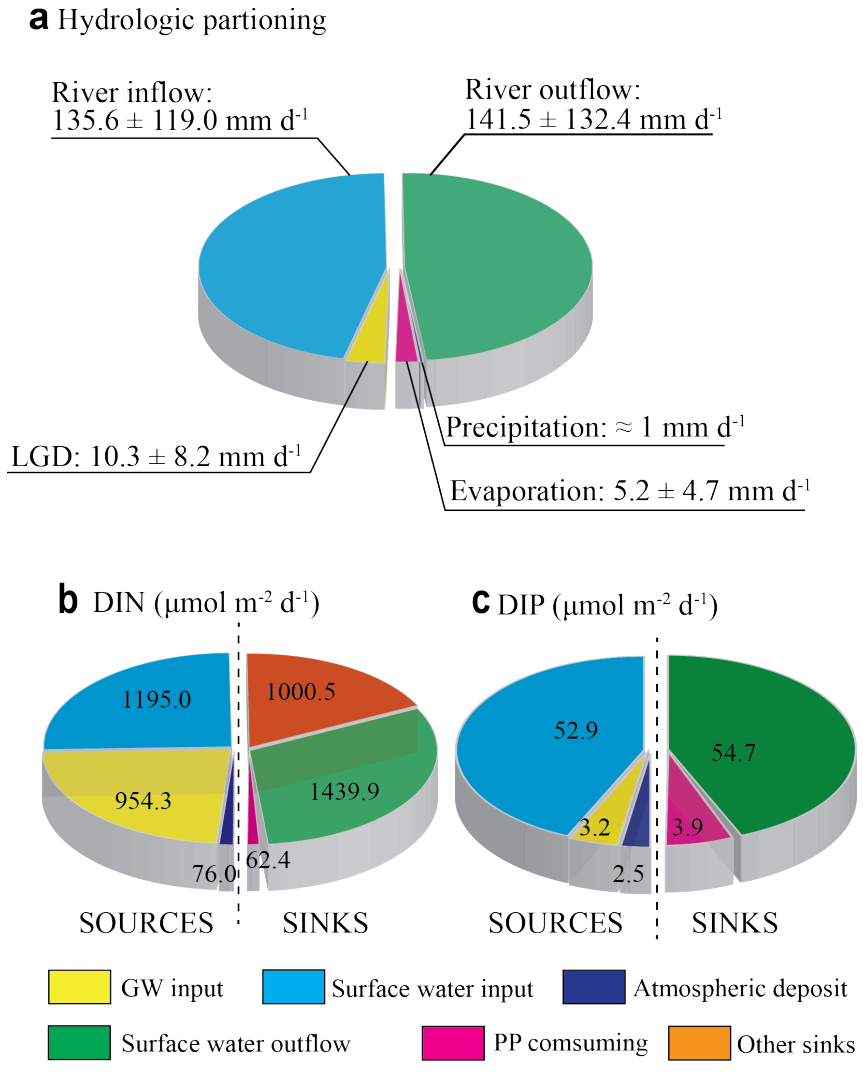

1100

Hydrol. Earth Syst. Sci. Discuss., https://doi.org/10.5194/hess-2018-26
Manuscript under review for journal Hydrol. Earth Syst. Sci.
Discussion started: 12 February 2018

Table 1 Parameters used to establish the mass balance model of ^{222}Rn in Ximen Co Lake.

Parameters	Units or values	Estimated Uncertainty (%)	Evaluation
Wind speed (ω_{10})	0.2 - 5.4 m s^{-1}	n.a	From Jiuzhi weather stations
Water-air temperature	11.2 - 15.6 ^{o}C	n.a	Recorded with probe in the chamber; sensitive to temperature results
Molecular diffusion of ^{222}Rn in water (D_m)	9.2×10^{-6} - 1.0×10^{-5} cm^2 s^{-1}	n.a	1.16×10^{-6} at 20 ^{o}C; adjustable for temperature
Molecular diffusion of ^{222}Rn in sediments (D_s)	2.2×10^{-6} - 2.5×10^{-5} cm^2 s^{-1}	n.a	Adjusted for temperature, sediment porosity
Dynamic viscosity (μ)	1.1×10^{-3} - $1.3\times10^{-3}$$cm^2$ s^{-1}	n.a	Calculated based on water temperature, density and salinity
Schmidt number (S_c)	1078.6 - 1371.6 [-]	n.a	Calculated as the ratio of υ to D_m
Water depth (H)	4.4 m	n.a	Epilimnion depth of Ximen Co Lake
Decay constant ^{222}Rn (λ_{222})	0.186 d^{-1}	n.a	Constant
Groundwater endmember ^{222}Rn (C_{gw})	11200 ± 1200 Bq m^{-3}	8 sites dependant for	Measured; final result for water flux inversely proportional to ^{222}Rn
Lake water endmember ^{222}Rn (C_l)	21.6- 418.8 Bq m^{-3}	15-25%	Measured with RAD 7 AQUA
Atmospheric ^{222}Rn (C_a)	1.5 ± 1.0 Bq m^{-3}	20-25%	Measured or assumed value, model not sensitive to radon in air variation
$K_{air/water}$	0.29 - 0.33 [-]	n.a	Calculated based on temperature in the chamber and salinity in lake water
Porosity n	0.31	n.a	Assumed based on literatures
Tortuosity θ	2.05	n.a	Calculated based on porosity
Piston velocity (κ)	0.004 - 1.11 m d^{-1}	20-25%	Calculated from Equation 3 in supplementary information
^{226}Ra concentration in lake waters (C_{226Ra})	0.01 Bq m^{-3}	≈10%	Measured with RAD7
Diffusive flux of ^{222}Rn (F_{diff})	0.68 - 213.5 Bq m^{-2} d^{-1}	n.a	Calculated from Equation 9 in supplementary information
Atmospheric flux of ^{222}Rn (F_{atm})	0.7 - 213.5 Bq m^{-2} d^{-1}	n.a	Calculated from Equation 1 in supplementary information
Groundwater flux of ^{222}Rn (F_{gw})	14.7 - 349.8 Bq m^{-2} d^{-1}	n.a	Calculated from Equation 1
Inventory of ^{222}Rn (I)	Bq m^{-2}	n.a	Measured with RAD7 AQUA
Groundwater discharge (Q_{gw})	10.3 ± 8.2 (3.5-38.6) mm d^{-1}	n.a	Calculated from Equation 1

Hydrol. Earth Syst. Sci. Discuss., https://doi.org/10.5194/hess-2018-26
Manuscript under review for journal Hydrol. Earth Syst. Sci.
Discussion started: 12 February 2018

Hydrology and Earth System Sciences
Discussions
Open Access
EGU

Table 2 Input parameters for the three endmember model of Ximen Co Lake

Input parameter	Description	Values (using ^{18}O as a tracer)	Parametric sources
h	Relatively humidity	0.63	Measured by the humidity meter
T (°C)	Water temperature	15.66	Monitored with divers
$\delta_{surface}$ (^{18}O) ‰	Surface water isotopic compositions	-12.45	Average value of surface inflow samples
δ_{gw} (^{18}O) ‰	Groundwater isotopic compositions	-11.97	Average value of porewater samples
δ_L (^{18}O) ‰	Lake water isotopic compositions	-12.54	Average value of Ximen Co Lake water samples
F_{gw} (mm/d)	LGD rates	14.18	Calculated based on ^{222}Rn mass balance model
ε^* (^{18}O) ‰	Effective equilibrium isotopic enrichment factor	10.12	Equations 13-14 in supplementary information
C_k (^{18}O) ‰	Kinetic constant for ^{18}O	14.2	Constants based on evaporating experiment
ε_k (^{18}O) ‰	Kinetic enrichment factor	5.2	From Equation 15 in supplementary information
ε (^{18}O) ‰	Total isotopic enrichment factor	15.33	The sum of $\varepsilon^*$and C_k
α^* (^{18}O) ‰	Effective isotopic equilibrium factor	1.01	$\alpha^*=1+\varepsilon^*$
δ_a (^{18}O) ‰	Isotopic composition of ambient air	-23.12	Estimated with δ_{in} and δ_a
δ_{in} (^{18}O) ‰	Isotopic composition of surface inflow water	-13.41	Average value of surface inflow water
δ_E (^{18}O) ‰	Isotopic compositions of evaporating vapor	-35.1	From Equation 12 in supplementary information
$[Cl]_{in}$ (mgL^{-1})	Chloride concentrations in surface inflow water	0.91	Filed data
$[Cl]_L$ (mgL^{-1})	Chloride concentrations in lake water	1.02	Filed data
$[Cl]_{gw}$ (mgL^{-1})	Chloride concentrations in groundwater	1.48	Filed data